Published for SISSA by Springer

Received: *July 20, 2023*
Revised: *November 23, 2023*
Accepted: *January 4, 2024*
Published: *January 23, 2024*

Study of charm hadronization with prompt Λ_c^+ baryons in proton-proton and lead-lead collisions at $\sqrt{s_{NN}} = 5.02$ TeV

The CMS collaboration

E-mail: cms-publication-committee-chair@cern.ch

Abstract: The production of prompt Λ_c^+ baryons is measured via the exclusive decay channel $\Lambda_c^+ \to p\mathrm{K}^-\pi^+$ at a center-of-mass energy per nucleon pair of 5.02 TeV, using proton-proton (pp) and lead-lead (PbPb) collision data collected by the CMS experiment at the CERN LHC. The pp and PbPb data were obtained in 2017 and 2018 with integrated luminosities of 252 and $0.607\,\mathrm{nb}^{-1}$, respectively. The measurements are performed within the Λ_c^+ rapidity interval $|y| < 1$ with transverse momentum (p_T) ranges of 3–30 and 6–40 GeV/c for pp and PbPb collisions, respectively. Compared to the yields in pp collisions scaled by the expected number of nucleon-nucleon interactions, the observed yields of Λ_c^+ with $p_T > 10$ GeV/c are strongly suppressed in PbPb collisions. The level of suppression depends significantly on the collision centrality. The Λ_c^+/D^0 production ratio is similar in PbPb and pp collisions at $p_T > 10$ GeV/c, suggesting that the coalescence process does not play a dominant role in prompt Λ_c^+ baryon production at higher p_T.

Keywords: Heavy Ion Experiments, Heavy Quark Production, Relativistic Heavy Ion Physics

ArXiv ePrint: 2307.11186

https://doi.org/10.1007/JHEP01(2024)128

JHEP01(2024)128

Contents

1 Introduction

In relativistic heavy ion collisions, hadrons containing a heavy quark are versatile probes for understanding parton energy loss and thermalization properties associated with the quark-gluon plasma (QGP) formed in these collisions [1–7]. Because of their large rest masses, heavy quarks are primarily produced in the initial hard scatterings and interact with the medium by different energy loss mechanisms than light-flavor quarks [8]. A thorough understanding of both the in-medium interactions and the subsequent hadronization processes is needed to correctly interpret the experimental data. In proton-proton (pp) collisions, hadronization is expected to occur in the form of a fragmentation process [9]. While the fragmentation process can still occur during heavy ion collisions, in these collisions hadrons can also form by parton coalescence inside or at the boundary of the QGP medium [10, 11]. The effect of coalescence is expected to be most prominent for low and intermediate transverse momentum (p_{T}) hadrons, for which the density is highest for the precursor partons. The coalescence probability decreases with increasing hadron p_{T}, leading to the dominance of the fragmentation process of hadronization at high p_{T}.

In the presence of a QGP, the parton coalescence contribution for baryon production is expected to be higher than that for meson production at a fixed hadron p_{T} value. This is a consequence of the hadron p_{T} value reflecting the sum of the constituent quark p_{T} values and of having a decreasing quark density with increasing quark p_{T}. In particular,

JHEP01(2024)128

a large enhancement in the Λ_c^+/D^0 yield ratio in heavy ion relative to pp collisions is predicted by models including the coalescence of charm and light-flavor quarks in Λ_c^+ baryon production [12–15], with the enhancement expected to have a strong p_T dependence.

The production of Λ_c^+ baryons for a variety of collision systems has been measured by RHIC and LHC experiments. At the LHC, Λ_c^+ p_T-differential cross section measurements have been made for pp collisions at midrapidity ($y \sim 0$) by ALICE [16, 17] and CMS [18], and at forward rapidity by LHCb [19]. These measurements are compared to theoretical predictions from the next-to-leading order general-mass variable-flavor-number scheme (GM-VFNS) [20, 21] and to PYTHIA8 with color reconnection [22]. Within the rapidity range 2.0–4.5, these predictions are consistent with the LHCb results. The GM-VFNS calculations, however, underestimate ALICE and CMS results for $|y| < 0.5$ and 1.0, respectively. The PYTHIA8 calculations with mode 2 of the color reconnection mechanism (CR2) [22] activated are in general agreement with the experimental results [17, 18]. ALICE and LHCb also report Λ_c^+/D^0 production ratios for pp and proton-lead (pPb) collisions. The ALICE ratios from pp and pPb collisions [16] are above the corresponding LHCb values [23], indicating a rapidity dependence for baryon and meson hadronization.

At RHIC, the STAR Collaboration measured Λ_c^+ production at midrapidity ($|y| < 1$) in gold-gold collisions at a center-of-mass energy per nucleon pair ($\sqrt{s_{_{NN}}}$) of 200 GeV [24]. In heavy ion collisions, measurements are often done in centrality classes that are given in percentage ranges of the total inelastic hadronic cross section, with the 0–20% centrality bin corresponding to the 20% of collisions having the largest overlap of the two nuclei. Within the 0–20% centrality range, the Λ_c^+/D^0 ratio for $3 < p_T < 6$ GeV/c is found to be significantly higher than predicted by the PYTHIA8 event generation model [25] for pp collisions. Also, an ALICE measurement of the Λ_c^+/D^0 ratio for $p_T < 10$ GeV/c at midrapidity in lead-lead (PbPb) collisions at 5.02 TeV [26, 27] finds larger values than those in pp and pPb collisions. In contrast, the CMS results in the higher-p_T range 10–20 GeV/c are consistent with the pp results [18]. The Λ_c^+ nuclear modification factor (R_{AA}) is the ratio of Λ_c^+ baryon yields in PbPb to the pp results scaled by the number of nucleon-nucleon (NN) binary collisions. The ALICE and CMS measurements of the R_{AA} at 5.02 TeV find this ratio to be less than unity, indicating a medium-induced charm quark energy loss before hadronization [16–18, 26, 27]. More information on the coalescence process in heavy flavor hadron production can be obtained from the recent LHC measurements at 5.02 TeV of X(3872) in PbPb collisions [28], and B_c^+ production in pp and PbPb collisions [29].

In this paper, we report on the measurements of prompt Λ_c^+ baryon production in 5.02 TeV pp and PbPb collisions with data collected using the CMS detector in 2017 and 2018, respectively. The integrated luminosities of the pp and PbPb data are 252 and 0.607 nb^{-1}, respectively [30–32]. The term "prompt Λ_c^+" is used to denote Λ_c^+ baryons that are either directly generated during charm quark hadronization or formed through the strong interaction decay of excited charmed hadron states [33]. This is in contrast to "nonprompt Λ_c^+", which refers to Λ_c^+ baryons that originate from the decay of b hadrons.

The Λ_c^+ baryons are reconstructed in the central rapidity region ($|y| < 1$) via the hadronic decay channel $\Lambda_c^+ \to pK^-\pi^+$. In pp collisions, the p_T spectrum is measured in the p_T range 3–30 GeV/c. The p_T spectrum and the R_{AA} are measured in the integrated

JHEP01(2024)128

centrality class of 0–90% with $6 < p_T < 40$ GeV/c and $6 < p_T < 30$ GeV/c, respectively. These are also measured in the centrality bins 0–10, 10–30, 30–50 and 50–90% within different p_T ranges. The Λ_c^+/D^0 production ratios are obtained for pp and PbPb collisions with $3 < p_T < 30$ GeV/c and $6 < p_T < 40$ GeV/c, respectively, using previously reported CMS results for D^0 production [34]. The PbPb Λ_c^+/D^0 ratio is also measured for the centrality class 0–10% in the p_T range 10–40 GeV/c. All references to Λ_c^+ and D^0 in the text of this paper also include the corresponding charge conjugate states. Tabulated results are provided in the HEPData record for this analysis [35].

2 The CMS apparatus

The central feature of the CMS apparatus is a superconducting solenoid of 6 m internal diameter, providing a magnetic field of 3.8 T. Within the solenoid volume, there is a silicon pixel and strip tracker that measures the trajectories of charged particles in the pseudorapidity range $|\eta| < 2.5$, a lead-tungstate crystal electromagnetic calorimeter, and a brass and scintillator hadron calorimeter. For charged particles of $1 < p_T < 10$ GeV/c and $|\eta| < 1.4$, the typical track resolution is 1.5% in p_T and 25–90 (45–150) μm in the transverse (longitudinal) impact parameter [36]. Two forward hadron (HF) calorimeters use steel as an absorber and quartz fibers as the sensitive material. The two HF calorimeters are located 11.2 m away from the interaction region, one on either side, and together they extend the calorimeter coverage to $3.0 < |\eta| < 5.2$. Each HF calorimeter consists of 432 readout towers consisting of a geometrically defined group of calorimeter cells. The HF calorimeter cells contain long and short quartz fibers running parallel to the beam that provide information on the shower energy and the relative contribution originating from hadrons versus electrons and photons. In this analysis, the HF information is used for performing an offline event selection and for determining event centrality. The Beam Pickup and Timing for LHC eXperiments (BPTX) provides precise information on the bunch structure and timing of the beam. A detailed description of the CMS experiment can be found in ref. [37].

3 Event selection and simulated event sample

Events are required to pass selection criteria designed to reject those arising from background processes such as beam-gas interactions and nonhadronic collisions, as described in ref. [38]. Events must have at least one reconstructed primary interaction vertex formed by two or more tracks [36] within a distance of 15 cm from the center of the nominal interaction region along the beam axis. In addition, in PbPb collisions, the shapes of the clusters in the pixel detector must be compatible with those expected from particles produced at the primary vertex location [39]. The PbPb collision events are also required to have at least two towers in each HF detector with energy deposits of more than 4 GeV per tower. This analysis processes PbPb minimum-bias (MB) and pp zero-bias (ZB) trigger events. The PbPb MB trigger requires signals on both sides of the HF calorimeters [40]. The number of interactions per bunch crossing in pp collisions is less than 5, and hence the ZB trigger is used in this analysis. The pp ZB trigger requires a coincidence of the signals from the BPTX detectors located on either side of the interaction point, indicating the presence of bunches from both beams at CMS.

JHEP01(2024)128

Monte Carlo (MC) simulated event samples for pp and PbPb collisions are used to optimize the selection criteria, calculate the acceptance times efficiency factors, estimate the systematic uncertainties, and facilitate the separation of prompt and nonprompt Λ_c^+ baryons. The pp MC samples are generated using PYTHIA8 2.1.2 [25], hereafter referred to as PYTHIA8, with tune CP5 [41], which includes both prompt and nonprompt Λ_c^+ baryon events. For the PbPb MC samples, each PYTHIA8 event containing a Λ_c^+ baryon is embedded into a PbPb collision event generated with HYDJET 1.9 [42], which is tuned to reproduce global event properties such as the charged-hadron p_T spectrum and particle multiplicity. The $\Lambda_c^+ \to pK^-\pi^+$ decay is simulated using EVTGEN 1.3.0 [43] based on four sub-channels: $\Lambda_c^+ \to p\overline{K}^*(892)^0 \to pK^-\pi^+$, $\Lambda_c^+ \to \Delta(1232)^{++}K^- \to pK^-\pi^+$, $\Lambda_c^+ \to \Lambda(1520)\pi^+ \to pK^-\pi^+$, and $\Lambda_c^+ \to pK^-\pi^+$ (nonresonant), with no modeling of interference between the sub-channels. Details of the decay channel and its subchannels can be found in ref. [44]. All particles are propagated through a simulation of the CMS detector response using the GEANT4 package [45].

4 Signal reconstruction and extraction

The signal is reconstructed by selecting three charged-particle tracks within $|\eta| < 1.2$ in the mass range 2.11–2.45 GeV/c^2. The net charge of $\Lambda_c^+ \to pK^-\pi^+$ candidates and their charge conjugates are required to be +1 and −1, respectively. All charged tracks must have $p_T > 0.5$ GeV/c and 1.0 GeV/c for pp and PbPb collisions, respectively. Signal events will have two same-sign tracks from a proton and a charged pion and an opposite-sign track for the kaon. Without particle identification, the possibilities for either of the same-sign tracks to be a proton or a pion are considered, with the kaon mass assumed for the opposite-sign track. The invariant mass distribution of the reconstructed signal with an incorrect mass assignment is much broader, about 30 times the width of the signal with the correct mass assignment. These misidentified events are indistinguishable from the combinatorial background and are thus treated as part of the background during signal extraction.

The raw signal yields are obtained in each p_T and centrality interval using unbinned maximum likelihood fits. The fit function consists of several components. To account for the variation of track momentum resolution as a function of rapidity, a double Gaussian function is used to model the signal shape in pp collisions, with a common mean value for the two Gaussians, but with different widths. The PbPb signal shape is modeled using a triple Gaussian function, again with a common mean value but different widths. The widths and the relative areas of the Gaussian functions are obtained from the fit to simulated signal. A Chebyshev polynomial function is used to model the combinatorial background underlying the Λ_c^+ signal including the background due to incorrect mass assignments for both pp and PbPb collisions. The order of the Chebyshev polynomial function for the nominal background shape is determined by a likelihood ratio test [46].

As the event multiplicities for pp and PbPb collisions are substantially different, the selection criteria were optimized separately. The selection criteria optimization procedure mostly follows the one described in ref. [18], except that a gradient-boosted decision tree (BDTG) is chosen as the classification method. The variables used in the training are: the χ^2 probability of vertex fit to the daughter tracks of Λ_c^+, the angle between the Λ_c^+ momentum and the vector connecting the production and decay vertices, the distance between the two

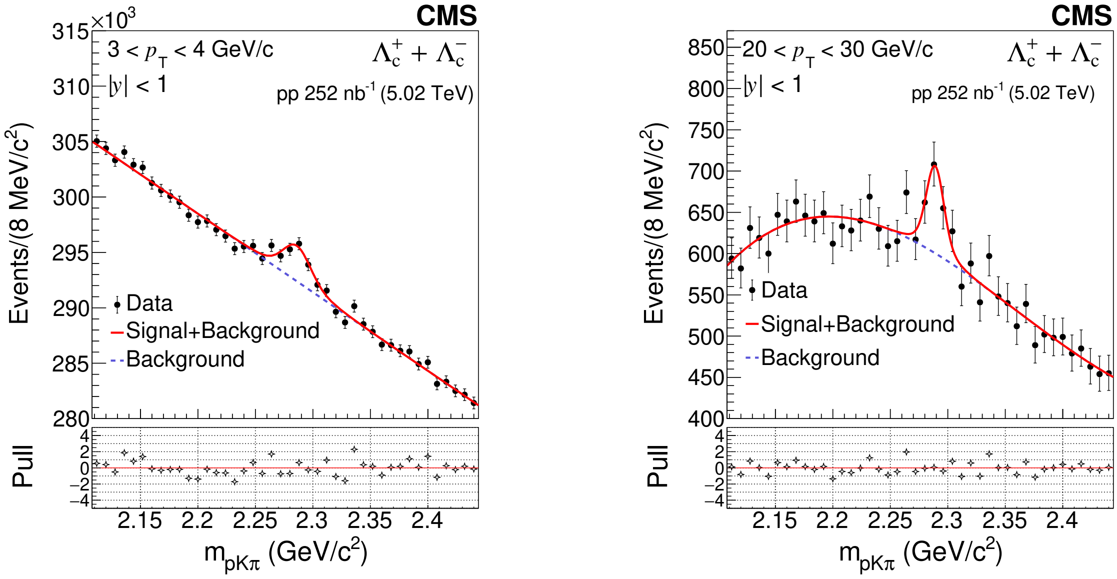

Figure 1. The number of reconstructed Λ_c^+ candidates per 8 MeV/c^2 invariant mass in pp collisions for p_T = 3–4 (left) and 20–30 GeV/c (right). The solid line represents the fit to the data and the dashed line represents the fit to the background. The lower panels show the pulls, obtained as the difference between the data points and the fit result, divided by the uncertainty in data.

vertices, and the ratio of the daughter track p_T to that of the Λ_c^+ candidate. The BDTG optimization is used for the full p_T range 3–30 GeV/c for pp collisions and in the range 6–10 GeV/c for PbPb collisions. In the p_T range 10–40 GeV/c for PbPb collisions, the selection criteria are optimized for individual variables, since the BDTG training leads to irregular shapes in the side band region of the mass distribution. When performing the signal extraction, the widths and relative yields for the multiple Gaussian functions are fixed to the values found using MC simulations. To account for the difference in the widths of the Gaussian functions in the simulation and data, each width of the multiple Gaussian function is multiplied by an additional common scaling factor, obtained by fitting the mass distribution. The mean of the signal function is treated as a fit parameter. The pull distributions (defined here as the ratio of the difference between the data and the model fit value to the uncertainty in data) show the behavior of a random variable that is consistent with a Gaussian distribution with zero mean and unit width, which indicates the absence of bias in the fitting procedure.

Figure 1 shows the invariant mass distribution of Λ_c^+ candidates in pp collisions for p_T = 3–4 (left) and 20–30 GeV/c (right). Figure 2 displays the invariant mass distribution of Λ_c^+ candidates for PbPb collisions with p_T = 6–8 (left) and 30–40 GeV/c (middle) in the 0–90% centrality bin, and for p_T = 10–12.5 GeV/c (right) in the 0–10% centrality bin. The solid line represents the fit to the data and the dashed line represents the contribution from the combinatorial background. For pp collisions, a clear Λ_c^+ signal peak is observed between p_T = 3–4 and 20–30 GeV/c. For PbPb collisions, a significant signal is observed between p_T = 6–8 and 30–40 GeV/c for the 0–90% centrality bin. For the 0–10% centrality bin, the lowest p_T bin with a clearly resolved signal peak is 10–12.5 GeV/c.

JHEP01(2024)128

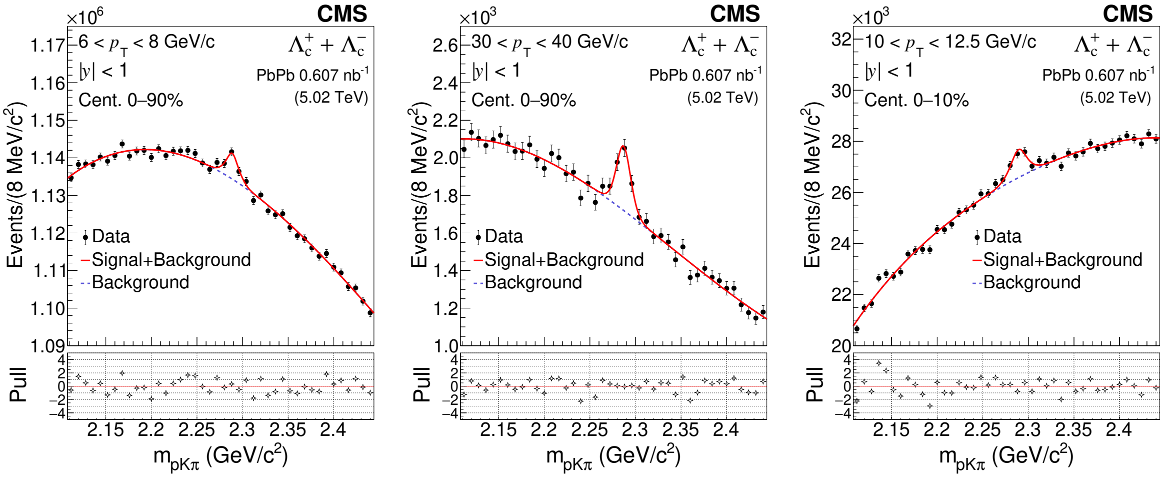

Figure 2. The number of reconstructed Λ_c^+ candidates per 8 MeV/c^2 invariant mass in PbPb collisions for $p_T = 6$–8 (left) and 30–40 GeV/c (middle) in the 0–90% centrality bin, and for $p_T = 10$–12.5 GeV/c in the 0–10% (right) centrality bin. The solid line represents the fit to the data and the dashed line represents the contribution from the combinatorial background. The lower panels show the pulls, obtained as the difference between the data points and the fit result, divided by the uncertainty in data.

5 Prompt signal fraction

The distribution of the distance of closest approach (DCA) of the inclusive Λ_c^+ particles is used to obtain the prompt Λ_c^+ fraction (f_{prompt}). For PbPb collisions, the DCA is defined as the closest three-dimensional distance between the Λ_c^+ particle and the primary vertex. In case of a single event containing tracks from multiple collisions, the DCA can be distorted when the Λ_c^+ does not originate from the primary vertex. To minimize this effect, the DCA for pp collisions is taken as the closest two-dimensional distance in the transverse plane between the trajectory of the Λ_c^+ particle and the beamline, taking advantage of the small transverse beam size. Compared to that for prompt Λ_c^+ particles, the nonprompt Λ_c^+ DCA distribution, which results from b hadron decays, is wider. Templates of prompt and nonprompt Λ_c^+ distributions based on MC signal simulation are used to fit the data with the relative yield of the two components as the fit parameter. The fits are done with different DCA resolutions applied to the MC template to accommodate the imperfect description of the data by the MC simulations. The result of the fit with the minimum χ^2 is chosen to be the nominal value of the prompt Λ_c^+ fraction. The prompt fractions for pp and PbPb collisions remain relatively constant over the measured p_T and centrality (for PbPb collisions) ranges, with values between 0.79–0.88 and 0.78–0.99, respectively. An exception occurs for PbPb collisions for the analysis bin corresponding to $p_T = 10$–12.5 GeV/c and 0–10% centrality. In this bin, the prompt ratio is 0.42 as a result of the tighter selection criteria. It is not feasible to obtain the DCA distribution from data for $p_T < 4$ and >15 GeV/c in pp collisions because of the small signal-to-background ratio and the limited number of events, respectively. For $p_T < 4$ GeV/c, the value of the neighboring p_T bin is used as the nominal value of the prompt Λ_c^+ fraction (0.85) and for individual bins with $p_T > 15$ GeV/c, the p_T bins are combined and the DCA fit is performed to obtain the nominal value (0.79).

JHEP01(2024)128

Model predictions are obtained using PYTHIA8 with CR2 [22] activated and fixed-order next-to-leading logarithmic (FONLL) calculations [47]. The FONLL calculation does not include the nonprompt Λ_c^+ cross section. The nonprompt component from FONLL is obtained by weighting the nonprompt Λ_c^+ cross section from PYTHIA8 with the ratio of the p_T-differential b hadron cross sections obtained from FONLL to that from PYTHIA8. The PYTHIA8 prediction overestimates the observed b hadron cross section over the full p_T range [48], while the FONLL prediction is much closer to the data. Therefore, the FONLL calculation is used to determine the systematic uncertainty related to the prompt fraction for $p_T < 4\,\text{GeV}/c$, as discussed in section 7.

6 Acceptance and efficiency

The product of the acceptance and efficiency ($A\epsilon$) is obtained from the MC simulation as a fraction in which the numerator is the number of reconstructed prompt Λ_c^+ candidates that pass the signal selection criteria and the denominator is the number of generated prompt Λ_c^+ baryons in the considered p_T bin and with $|y| < 1$. Since there are four sub-channels in the $\Lambda_c^+ \to pK^-\pi^+$ decay, $A\epsilon$ is the weighted average of the four sub-channels according to their branching fractions. There is a slight discrepancy between the observed and simulated collision vertex distribution along the beam direction (V_z) for both pp and PbPb collisions. A small discrepancy also exists with the centrality distribution of the events in PbPb collisions. The discrepancy in the V_z distribution is addressed by a weight factor that is the ratio of the V_z distribution of data to that of the MC simulation. The discrepancy in the centrality distributions is addressed by a weight factor given by the ratio of the centrality distribution of data to that of the MC simulation multiplied with the average number of NN binary collisions ($\langle N_{coll} \rangle$). The values of $\langle N_{coll} \rangle$ are calculated using a MC Glauber model [49]. The p_T spectrum of the generated Λ_c^+ baryons in the MC simulation is also weighted to match the data for both pp and PbPb collisions. This weighting procedure is done iteratively until sequential values of $A\epsilon$ converge. The distributions of variables used for the selection criteria optimization are shifted in the MC simulation so that the probability of having a Λ_c^+ candidate with a value equal to or lower than the nominal value in the data distribution is equivalent to the probability of having a candidate with a value equal to or lower than the adjusted value in the original MC distribution, before the $A\epsilon$ value is calculated.

Figure 3 displays the $A\epsilon$ value as a function of p_T for prompt Λ_c^+ in pp and PbPb collisions. For the same p_T value in PbPb collisions, the $A\epsilon$ value decreases toward more central collisions as a result of tighter selection criteria. Within the same centrality range, the $A\epsilon$ values increase from low to high p_T, mostly because of the longer average decay length of high p_T particles. The $A\epsilon$ values for pp collisions are significantly higher than those for PbPb collisions because of a smaller combinatorial background allowing for more relaxed selection criteria. The decrease in the $A\epsilon$ values for $p_T > 20\,\text{GeV}/c$ in pp collisions results from tighter selection criteria.

JHEP01(2024)128

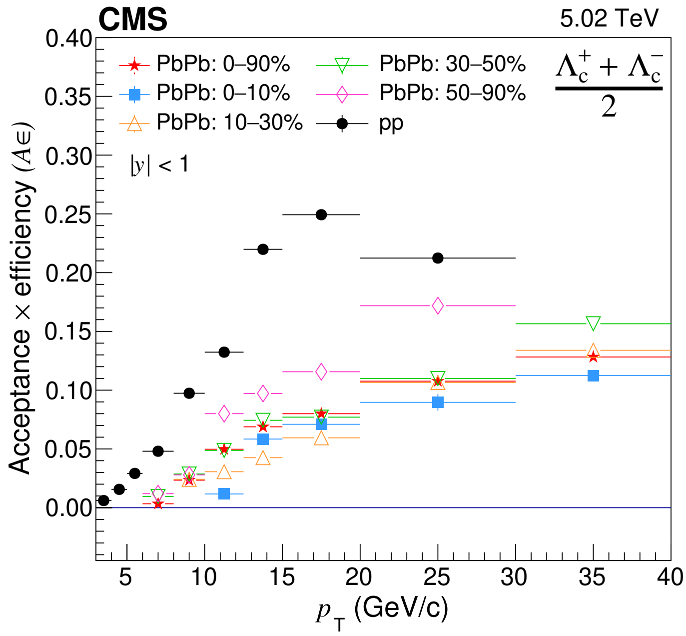

Figure 3. The product of acceptance and efficiency ($A\epsilon$) as a function of p_T for prompt Λ_c^+ in pp and PbPb collisions. The closed circles represent the value for pp. The $A\epsilon$ values for PbPb collisions in centrality bins 0–90, 0–10, 10–30, 30–50 and 50–90% are represented by symbols of star, square, triangle, inverted triangle, and diamond, respectively. The horizontal error bars represent the bin widths.

7 Sources of systematic uncertainty

The systematic uncertainties come from the extraction of the raw signal yield, the ability of the MC simulation to reproduce the data when varying selection criteria and in generating p_T spectra, the determination of prompt fraction from the raw signal yield, the branching fraction of the decay mode, and the integrated luminosity. Unless otherwise indicated, systematic uncertainties are combined by adding the individual contributions in quadrature. The systematic uncertainties mentioned here include the uncertainties for each p_T bin for pp collisions and the uncertainties for each p_T and centrality bin for PbPb collisions.

The systematic uncertainty in the raw signal yields is obtained by varying the modeling functions that are used for the signal and background contributions, as well as the fit range. The background function is changed from the default order to the next order Chebyshev polynomial, with the difference in yield between the alternative and the default fit functions taken as the systematic uncertainty. The uncertainties lie between 1–20% for pp collisions, and up to 34% for PbPb collisions. The signal yield uncertainty is largest for pp collisions with $p_T = 3$–$4\,\mathrm{GeV}/c$ and for 0–10% centrality PbPb collisions with $p_T = 12.5$–$15\,\mathrm{GeV}/c$. The systematic uncertainty from the signal shape is estimated by changing from the default to an alternative signal fit function while keeping the background polynomial function the same as for the default fit. As alternative signal fit functions, three and two Gaussians are used for pp and PbPb collisions, respectively. The difference in the signal yield obtained with the default and alternative functions is taken as the systematic uncertainty, which is less than

6% and 7% for pp and PbPb collisions, respectively. The systematic uncertainty from the fit range is estimated by changing the fit range from the default mass range 2.11–2.45 GeV/c^2 to alternative mass ranges of 2.17–2.37 and 2.15–2.41 GeV/c^2, for both pp and PbPb collisions. This leads to uncertainties within 2–26% and 1–24% for pp and PbPb collisions, respectively. The uncertainty is largest for pp collisions with $p_{\mathrm{T}} = 4$–$5\,\mathrm{GeV}/c$ and for 0–10% centrality PbPb collisions with $p_{\mathrm{T}} = 12.5$–$15\,\mathrm{GeV}/c$.

The uncertainties associated with a particular selection criterion, such as the BDTG cut value, are determined from a double ratio defined as

$$\mathcal{DR} = \frac{N_{\mathrm{Data}}(\mathrm{varied})}{N_{\mathrm{Data}}(\mathrm{nominal})} \bigg/ \frac{N_{\mathrm{MC}}(\mathrm{varied})}{N_{\mathrm{MC}}(\mathrm{nominal})}\,, \tag{7.1}$$

where $N_{\mathrm{Data}}(\mathrm{nominal})$ and $N_{\mathrm{Data}}(\mathrm{varied})$ are the yields obtained from data using the default and alternative selection criteria, respectively, and $N_{\mathrm{MC}}(\mathrm{nominal})$ and $N_{\mathrm{MC}}(\mathrm{varied})$ are the corresponding yields from the simulated events. The distribution of each selection criterion from MC is shifted so that the probability of a particular value for the Λ_{c}^{+} candidate is the same in the MC simulation as in the data. The associated systematic uncertainty is then based on the sensitivity of the $\mathcal{DR}$ for a particular selection criterion to changes in this criterion [18]. For pp and PbPb collisions, the uncertainties are found to be less than 6% and within 5–20%, respectively. The uncertainty is largest for 0–90% centrality PbPb collisions with $p_{\mathrm{T}} = 30$–$40\,\mathrm{GeV}/c$.

The difference between the experimental and MC Λ_{c}^{+} p_{T} distributions leads to an uncertainty when estimating $A\epsilon$. For both pp and PbPb collisions, this resulting uncertainty is taken as the difference in the estimated $A\epsilon$ value when using the experimental p_{T} distribution and the corresponding PYTHIA8 distribution with CR2 turned on. The resulting systematic uncertainty is up to 4% and 2% for pp and PbPb collisions, respectively.

The accuracy of the calculated $A\epsilon$ value also depends on knowledge of the resonant substructure of the $\mathrm{pK}^{-}\pi^{+}$ decay mode [44]. The calculation of $A\epsilon$ uses the appropriately weighted sum of the four known sub-channels. Pseudo-experiments are used to determine the distribution of $A\epsilon$ by randomly sampling the value of the branching fraction based on the corresponding uncertainty for each sub-channel. The systematic uncertainty is obtained as the standard deviation of a Gaussian fit to the $A\epsilon$ distribution and varies from 8–9% for pp and PbPb events.

The uncertainty of the single-track reconstruction efficiency is 2% for pp collisions and 5% for PbPb collisions [50]. Since there are three tracks in the Λ_{c}^{+} decay, the corresponding uncertainties on the measured p_{T} spectra are 6 and 15% for pp and PbPb collisions, respectively, assuming that the track efficiencies are correlated. The prompt D^{0} cross section measured using pp collision data collected in 2015 [34] is used to calculate the $\Lambda_{\mathrm{c}}^{+}/\mathrm{D}^{0}$ production ratio in this analysis. Since the uncertainty in the single track reconstruction for that analysis is 4%, we use this larger value when calculating the $\Lambda_{\mathrm{c}}^{+}/\mathrm{D}^{0}$ uncertainty for pp collisions. The uncertainties of reconstructing kaon and pion daughter tracks from D^{0} and Λ_{c}^{+} cancel, leading to the uncertainties from this source to be 4% in pp collisions and 5% in PbPb collisions as a result of the proton daughter track.

The uncertainties arising from the prompt fraction determination for most p_{T} bins are estimated by comparing the value obtained from the DCA distribution and the DCA significance

JHEP01(2024)128

distribution of the signal. The DCA significance is defined as the ratio of DCA to DCA uncertainty. The consistency between the data and MC in DCA significance is better than in DCA because the discrepancy between MC and data for the DCA and the DCA uncertainty partially cancel. The difference in the prompt fraction obtained from the two methods is treated as the systematic uncertainty of the prompt fraction. For $p_{\mathrm{T}} < 4\,\mathrm{GeV}/c$, the systematic uncertainty is calculated as the difference between the nominal value and FONLL predictions. For $p_{\mathrm{T}} > 15\,\mathrm{GeV}/c$, the difference between the prompt fraction obtained from DCA and the DCA significance for $12.5 < p_{\mathrm{T}} < 30\,\mathrm{GeV}/c$ is taken as the systematic uncertainty. The systematic uncertainty from this source is within 6–16% and up to 43% for pp and PbPb collisions, respectively. The uncertainty is largest for 30–50% centrality PbPb collisions with $p_{\mathrm{T}} = 30$–$40\,\mathrm{GeV}/c$.

The overall $\Lambda_c^+ \to pK^-\pi^+$ branching fraction uncertainty is 5% [44]. The uncertainties in the integrated luminosity for pp collisions and the MB selection efficiency for PbPb collisions are 2 and 1%, respectively. The uncertainties in the mean nuclear overlap function, $\langle T_{\mathrm{AA}} \rangle$, for PbPb collisions are between 2–5%. The $\langle T_{\mathrm{AA}} \rangle$ value is used in the calculation of R_{AA} and the T_{AA}-scaled Λ_c^+ yields for PbPb collisions, as discussed in section 8. The uncertainty based on the centrality calibration is obtained by varying the centrality bin edges by $\pm 0.5\%$, and taking the maximum relative difference with the default signal yield. The systematic uncertainty associated with the centrality calibration in PbPb collisions is up to 12%. The uncertainty is largest for 30–50% centrality PbPb collisions with $p_{\mathrm{T}} = 15$–$20\,\mathrm{GeV}/c$.

For the measurement of the p_{T} spectra, the uncertainties associated with the $\Lambda_c^+ \to pK^-\pi^+$ branching fraction, luminosity, tracking efficiency, and MB selection are taken as global ones. Adding these systematic uncertainty contributions in quadrature yields the global uncertainties of 8.6 and 15.9% for pp and PbPb collisions, respectively. When determining R_{AA} values, the uncertainties associated with the branching fraction and subresonant contributions cancel. The uncertainties associated with the D^0 yields from the yield extraction, selection criteria efficiency, and p_{T} shape, when calculating the Λ_c^+/D^0 production ratio, are obtained from ref. [34]. The uncertainties in tracking efficiency and in the branching fractions of Λ_c^+ and D^0 are included in the global systematic uncertainty for Λ_c^+/D^0 production ratio. The global uncertainty is 7% for both pp and PbPb collisions. The sources of the systematic uncertainties are summarized in table 1.

8 Results

The p_{T}-differential cross section for pp collisions is defined as:

$$\left.\frac{\mathrm{d}\sigma_{\mathrm{pp}}^{\Lambda_c^+}}{\mathrm{d}p_{\mathrm{T}}}\right|_{|y|<1} = \frac{f_{\mathrm{prompt}}}{2\mathcal{L}\Delta p_{\mathrm{T}}\mathcal{B}} \frac{N_{\mathrm{pp}}^{\Lambda_c^+}|_{|y|<1}}{A\epsilon}, \tag{8.1}$$

where $N_{\mathrm{pp}}^{\Lambda_c^+}|_{|y|<1}$ is the Λ_c^+ raw yield extracted in a p_{T} interval with $|y| < 1$, $\mathcal{L}$ is the luminosity of ZB events, Δp_{T} is the width of the p_{T} interval, f_{prompt} is the prompt Λ_c^+ fraction, $\mathcal{B}$ is the branching fraction of the decay channel, and the factor of 1/2 accounts for measurements of yields for both particles and antiparticles, but quoting the cross section for only particles. Figure 4 shows the p_{T}-differential cross sections for prompt Λ_c^+ baryon production in pp

JHEP01(2024)128

Sources of systematic uncertainties	pp	PbPb
Signal extraction (background)	1–20%	<34%
Signal extraction (signal)	<6%	<7%
Signal extraction (fit range)	2–26%	1–24%
Selection efficiency	<6%	5–20%
T_{AA}	—	2–5%
MC p_{T} shape	<4%	<2%
$A\epsilon_{\mathrm{reco}}$	8–9%	
Tracking efficiency	6%	15%
Prompt fraction	6–16%	<43%
Branching fraction	5%	
Integrated luminosity	2%	—
Minimum bias selection efficiency	—	1%
Centrality calibration	—	<12%

Table 1. Systematic uncertainties from different sources.

collisions with $|y| < 1$. The global 8.6% normalization uncertainty for the pp results is not included in the boxes representing the systematic uncertainties for each data point. The data are well described by PYTHIA8 after activating CR2 in which the final partons in the string fragmentation are considered to be color connected in such a way that the total string length becomes as short as possible [22]. The cross sections are also compared to the GM-VFNS perturbative QCD calculations [21, 51], which utilize fragmentation functions obtained by fitting data from the OPAL and Belle Collaborations [52, 53]. The GM-VFNS models, implementing fragmentation functions that are fitted to the OPAL data, only, and to both the OPAL and the Belle data are shown as GM-VFNS-1 and GM-VFNS-2, respectively. The error bars on the GM-VFNS predictions account for the renormalization scale uncertainty. The GM-VFNS predictions, which include both prompt and nonprompt baryon production, are systematically below our data for $p_{\mathrm{T}} < 8\,\mathrm{GeV}/c$, similar to the difference found by previous ALICE [16] and CMS measurements [18]. The DCA distribution fit of the data shows that ~20% of the generated Λ_c^+ baryons arise from b hadrons in the p_{T} range 3–30 GeV/c. Therefore, accounting for the effects of nonprompt Λ_c^+ production slightly enhances the disagreement with the data. The discrepancies in the cross sections and the Λ_c^+/D^0 production ratio [18] between the data and the GM-VFNS calculations in pp collisions indicate a breakdown of the universality of charm quark to hadron fragmentation functions.

The mean nuclear overlap function, $\langle T_{\mathrm{AA}} \rangle$, is equal to the average number of NN binary collisions ($\langle N_{\mathrm{coll}} \rangle$) divided by the pp inelastic cross section and can be interpreted as the NN-

JHEP01(2024)128

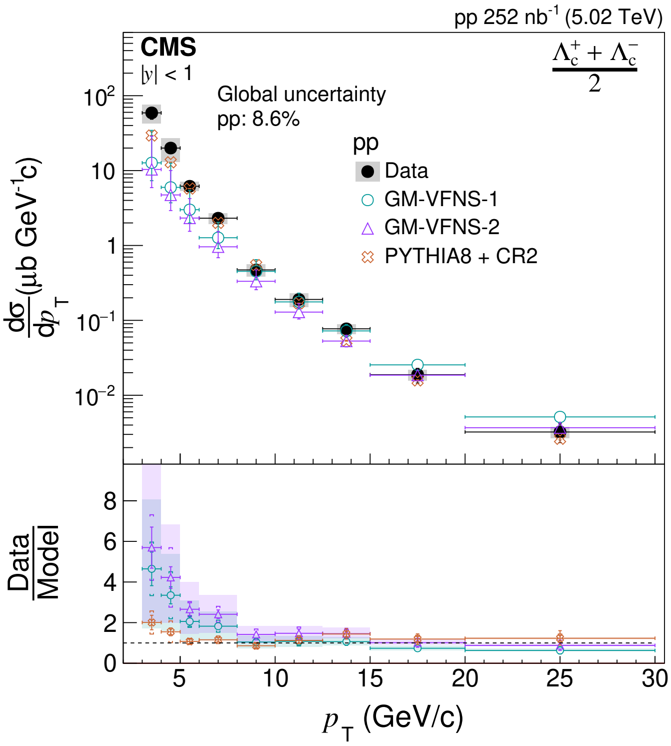

Figure 4. The p_{T}-differential cross sections for prompt Λ_c^+ production in pp collisions. Predictions for pp collisions are displayed for PYTHIA8 with CR2 (open crosses), GM-VFNS implementing fragmentation functions that are fitted to the OPAL data, only (open circles labeled GM-VFNS-1), and fitted to both OPAL and Belle data (open triangles labeled GM-VFNS-2). The GM-VFNS model calculations are for inclusive Λ_c^+ production. The horizontal error bars represent the bin widths. The vertical lines in the data points represent the statistical uncertainties and the shaded boxes represent the systematic uncertainties. The vertical lines in the model points represent the GM-VFNS uncertainties. The lower panel shows the data-to-prediction ratio for pp collisions with error bars and brackets corresponding to the statistical and total uncertainties in the data, respectively. The global fit uncertainty of 8.6% is not shown in the plot. The shaded boxes in the lower panel represent the GM-VFNS uncertainties.

equivalent integrated luminosity per heavy ion collision. The T_{AA}-scaled yields are defined as:

$$\frac{1}{\langle T_{\mathrm{AA}}\rangle}\frac{\mathrm{d}N^{\Lambda_c^+}_{\mathrm{PbPb}}}{\mathrm{d}p_{\mathrm{T}}}\Bigg|_{|y|<1} = \frac{f_{\mathrm{prompt}}}{\langle T_{\mathrm{AA}}\rangle}\frac{1}{2N_{\mathrm{events}}\Delta p_{\mathrm{T}}\mathcal{B}}\frac{N^{\Lambda_c^+}_{\mathrm{PbPb}}|_{|y|<1}}{A\epsilon}\,, \tag{8.2}$$

where N_{events} is the number of MB events. The other variables refer to the same physical quantities as in eq. (8.1). Figure 5 displays the T_{AA}-scaled yields for PbPb collisions in centrality bins of 0–90, 0–10, 10–30, 30–50 and 50–90% with $p_{\mathrm{T}} < 40\,\mathrm{GeV}/c$ and $|y| < 1$. The lowest p_{T} values for the measurements vary with centrality as the number of events and the signal-to-background ratio change, with thresholds of $6\,\mathrm{GeV}/c$ in the 0–90, 30–50 and 50–90% centrality bins, $8\,\mathrm{GeV}/c$ in the 10–30% bin, and $10\,\mathrm{GeV}/c$ in the 0–10% bin. The 15.9% normalization uncertainty for the PbPb results is not included in the boxes representing the systematic uncertainties. The pp measurement is included in the figure for comparison. Compared to the Λ_c^+ p_{T}-differential cross sections for pp collisions, the T_{AA}-scaled Λ_c^+ yields

JHEP01(2024)128

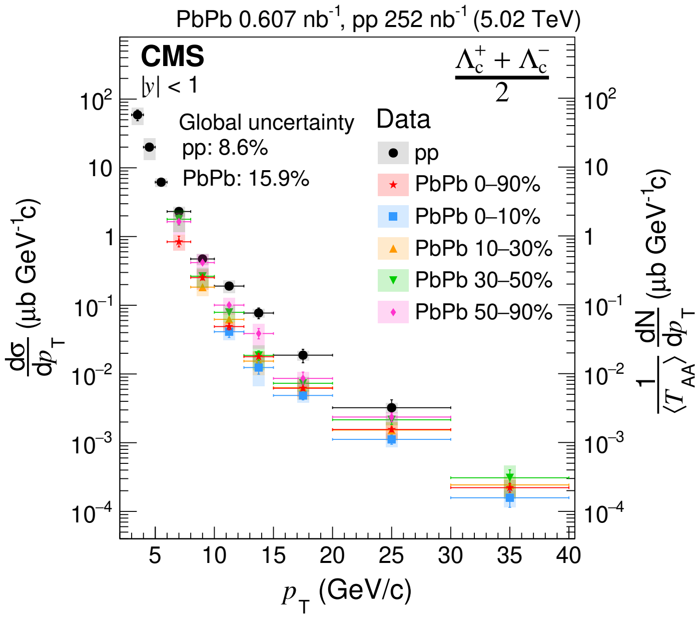

Figure 5. The p_T-differential cross sections for prompt Λ_c^+ production in pp collisions (circles) and the T_{AA}-scaled yields for PbPb collisions within centrality regions of 0–90 (stars), 0–10 (squares), 10–30 (triangles), 30–50 (inverted triangles) and 50–90% (diamonds) in PbPb collisions. The boxes and error bars represent the systematic and statistical uncertainties, respectively. The horizontal error bars represent the bin widths.

for PbPb collisions are systematically lower, with the reduction becoming more significant toward central collisions.

The R_{AA} value is used to quantify the suppression in production yield per NN collisions in PbPb relative to pp collisions. The Λ_c^+ R_{AA} value for PbPb collisions is defined as

$$R_{AA}(p_T) = \frac{1}{\langle T_{AA}\rangle}\frac{dN_{PbPb}^{\Lambda_c^+}}{dp_T}\Bigg/\frac{d\sigma_{pp}^{\Lambda_c^+}}{dp_T} . \tag{8.3}$$

Figure 6 shows the R_{AA} values for Λ_c^+ as a function of p_T for PbPb collisions within centrality regions of 0–90, 0–10, 10–30, 30–50 and 50–90% in $|y| < 1$. A larger suppression factor in Λ_c^+ production per NN collision is observed for more central PbPb collisions. Comparisons with the ALICE measurements [27], which extend to lower p_T values, for the 0–10 and 30–50% centrality ranges are displayed in figure 8 (in appendix A). The results suggest that the Λ_c^+ R_{AA} values are smallest near $p_T \approx 14\,\text{GeV}/c$, with larger values found at both lower and higher p_T. The trend is, in general, consistent with the observation from other heavy flavor hadron measurements, although the p_T of the minimum R_{AA} is different. For instance, the R_{AA} reaches a minimum at $p_T \approx 8\,\text{GeV}/c$ for nonprompt D^0 from b hadron decay and at $p_T \approx 9\,\text{GeV}/c$ for prompt D^0 [54].

The Λ_c^+/D^0 production ratio as a function of p_T for pp collisions and in the 0–90 and 0–10% centrality ranges for PbPb collisions in $|y| < 1$ are shown in figure 7. The ratio is calculated using the prompt Λ_c^+ measurements in this analysis and the previous CMS measurement for prompt D^0 mesons [34]. The purple curve in figure 7(left) represents the

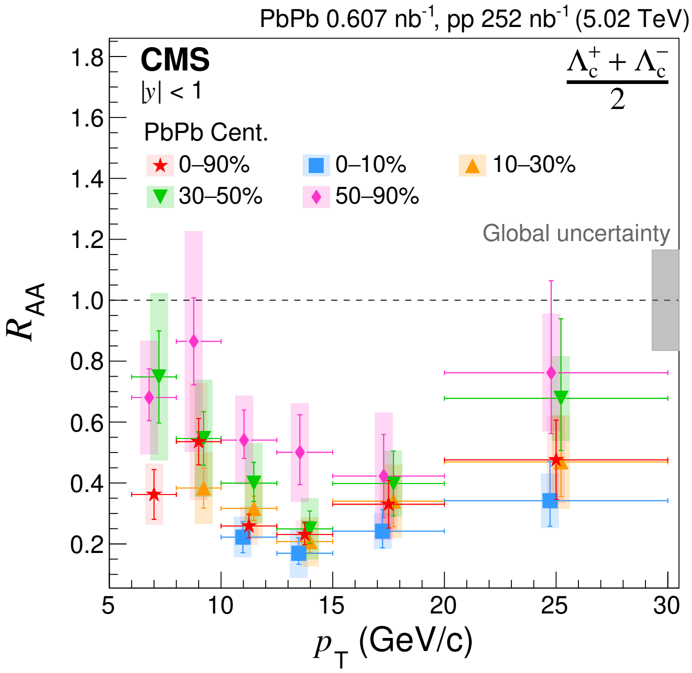

Figure 6. The nuclear modification factor R_{AA} versus p_{T} for prompt Λ_c^+ production in centrality regions of 0–90 (stars), 0–10 (squares), 10–30 (triangles), 30–50 (inverted triangles) and 50–90% (diamonds) in PbPb collisions. The mean position of the data points are shifted along the horizontal axis for clarity. The boxes and error bars represent the systematic and statistical uncertainties, respectively. The horizontal error bars represent the bin widths. The band at unity labeled global uncertainty includes the uncertainties for the luminosity of pp collisions, the number of MB events in PbPb collisions, and the tracking efficiency. The global uncertainty for R_{AA} is 16.5%.

prediction of PYTHIA8 with CR2 [22]. This prediction is consistent with our measurement in pp collisions for $p_{\mathrm{T}} < 10\,\mathrm{GeV}/c$, and is systematically lower than observed for $10 < p_{\mathrm{T}} < 30\,\mathrm{GeV}/c$. Two model calculations of the prompt Λ_c^+/D^0 ratio are also compared to the pp data. The dark blue band in figure 7(left) represents the updated prediction from a model, labeled as PLB821(2021)136622 in the figure, that includes both coalescence and fragmentation processes in pp collisions [55]. The update consisted in improvements on a previous calculation [15] that predicted a stronger dependence on p_{T} and underestimated the earlier CMS measurements [18]. The improvements include raising the underlying charm quark distribution to be closer to the upper limit of the FONLL prediction, and updating the charm fragmentation function to reproduce data for $p_{\mathrm{T}} > 10\,\mathrm{GeV}/c$. The new calculation describes the data very well for $p_{\mathrm{T}} < 10\,\mathrm{GeV}/c$. Another model [33], labeled as PLB795(2019)117 in figure 7(left), uses a statistical hadronization approach and explains the large Λ_c^+/D^0 production ratio as arising from Λ_c^+ baryons that are produced from the decay of excited charm baryon states not included in the particle data group (PDG) ref. [44] and therefore not included in the hadronization simulation in PYTHIA8. This model calculation, shown by the light yellow band, provides a reasonable description of the data for $p_{\mathrm{T}} < 12\,\mathrm{GeV}/c$.

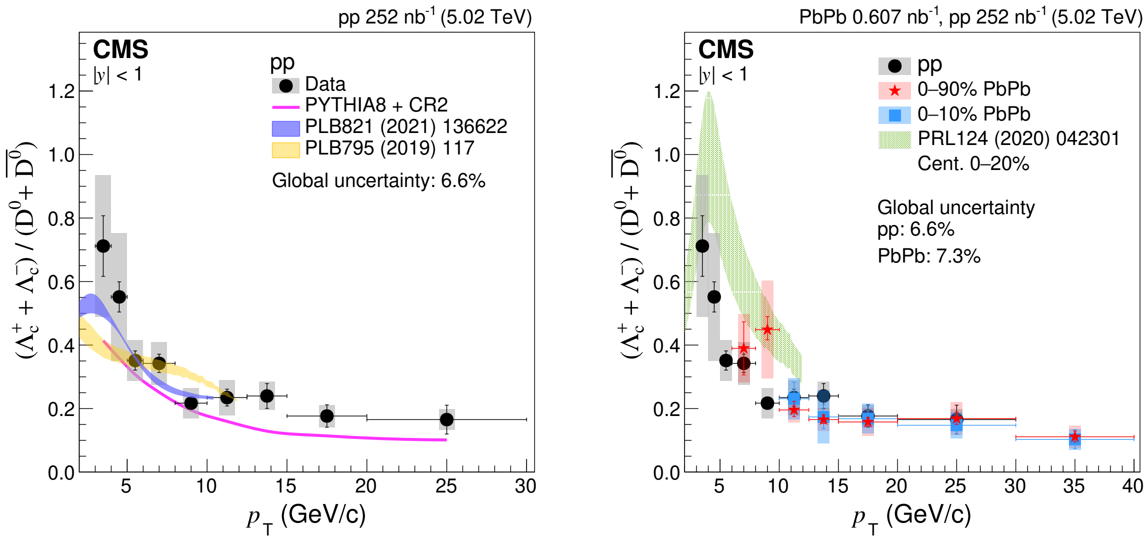

Figure 7. The ratio of the production cross sections of prompt Λ_c^+ to prompt D^0 versus p_T from pp collisions is represented by closed circles (left). The ratio for 0–90 (closed stars) and 0–10% (closed squares) centrality classes of PbPb collisions are compared to the pp result (right). The boxes and error bars represent the systematic and statistical uncertainties, respectively. The horizontal error bars represent the bin widths. The 6.6 and 7.3% normalization uncertainties in pp and PbPb collisions, respectively, are not included in the boxes representing the systematic uncertainties for each data point. Model calculations are displayed (see text for details).

The measurements of the Λ_c^+/D^0 ratio in 0–90 and 0–10% PbPb collisions with $p_T > 10\,\text{GeV}/c$ are consistent with the pp result. The Λ_c^+/D^0 ratios in pp and PbPb collisions approach the value found for e^+e^- collisions [18, 41] in this higher-p_T region. This lack of enhancement suggests that there is no significant contribution from the coalescence process in this p_T region for PbPb collisions. For $p_T < 10\,\text{GeV}/c$ and 0–90% centrality, the significance of the current measurement is not high enough to draw a definite conclusion. For $p_T > 10\,\text{GeV}/c$ and with centrality in the 0–10% range, the results are consistent with those of the ALICE Collaboration [27], as shown in figure 9 (in appendix A). The measurements of the Λ_c^+/D^0 production ratio in 0–10% PbPb collisions are also compared to a model calculation [56], represented by the light green band in figure 7(right). The model uses a four-momentum conserving recombination mechanism for baryons and applies space-momentum correlations between charm quarks and the hydrodynamical medium on an event-by-event basis. It also includes the decays of excited charm baryon states not included in ref. [44]. Although the calculation is done for the 0–20% centrality bin, the prediction for 0–10% is almost identical and consistent with the data within uncertainties for $10 < p_T < 12.5\,\text{GeV}/c$.

9 Summary

The differential cross section of prompt Λ_c^+ baryons as a function of transverse momentum (p_T) is presented for both proton-proton (pp) and lead-lead (PbPb) collisions at a center-of-mass energy per nucleon pair of 5.02 TeV in the central rapidity region $|y| < 1$. The measured p_T ranges are 3–30 GeV/c and 6–40 GeV/c for the pp and PbPb collisions, respectively. The

JHEP01(2024)128

p_{T} range of the pp and PbPb results, together with the differential centrality study of the prompt Λ_c^+ production, significantly extend previous CMS results based on 2015 data that was obtained with a lower integrated luminosity. The Λ_c^+ baryon yields for pp collisions are much higher than predicted by calculations with the general-mass variable-flavor-number scheme that use fragmentation functions obtained by fitting results from the OPAL and Belle Collaborations, indicating a breakdown of the universality of charm quark fragmentation functions. The nuclear modification factors, which correspond to the Λ_c^+ yields divided by the pp yields scaled up by the number of nucleon-nucleon collisions, have been measured in various centrality classes for the PbPb collisions. The prompt Λ_c^+ production for PbPb collisions is significantly suppressed compared to the pp collision results. The suppression magnitude is larger in more central collisions and shows a hint of varying with the Λ_c^+ baryon p_{T}. This is consistent with the partonic energy loss affecting charm quarks in the quark-gluon plasma. A similar effect was previously observed for (charmed) D^0 mesons and many other hadrons. The Λ_c^+/D^0 production ratio is measured for pp collisions with p_{T} in the range 3–30 GeV/c, 0–90% centrality PbPb collisions with p_{T} in the range 6–40 GeV/c, and 0–10% centrality PbPb collisions with p_{T} in the range 10–40 GeV/c. Calculations based on the event generator PYTHIA8 for the Λ_c^+/D^0 production ratio with the inclusion of color reconnection (mode 2) in the hadronization step can describe the pp data well for $p_{\mathrm{T}} < 10$ GeV/c, but are systematically lower for $10 < p_{\mathrm{T}} < 30$ GeV/c. A model taking into account the contributions from the decays of excited charm baryons and a model involving both coalescence and fragmentation can also describe the Λ_c^+/D^0 production ratios in pp collisions. For $p_{\mathrm{T}} > 10$ GeV/c, the Λ_c^+/D^0 ratios for pp and PbPb collisions are consistent with each other and approach the value found for $\mathrm{e}^+\mathrm{e}^-$ collisions, suggesting that the coalescence process does not play a significant role in Λ_c^+ baryon production in this higher-p_{T} region.

Acknowledgments

We thank Denes Molnar for his aid in improving the efficiency of the analysis computations.

We congratulate our colleagues in the CERN accelerator departments for the excellent performance of the LHC and thank the technical and administrative staffs at CERN and at other CMS institutes for their contributions to the success of the CMS effort. In addition, we gratefully acknowledge the computing centers and personnel of the Worldwide LHC Computing Grid and other centers for delivering so effectively the computing infrastructure essential to our analyses. Finally, we acknowledge the enduring support for the construction and operation of the LHC, the CMS detector, and the supporting computing infrastructure provided by the following funding agencies: SC (Armenia), BMBWF and FWF (Austria); FNRS and FWO (Belgium); CNPq, CAPES, FAPERJ, FAPERGS, and FAPESP (Brazil); MES and BNSF (Bulgaria); CERN; CAS, MoST, and NSFC (China); MINCIENCIAS (Colombia); MSES and CSF (Croatia); RIF (Cyprus); SENESCYT (Ecuador); MoER, ERC PUT and ERDF (Estonia); Academy of Finland, MEC, and HIP (Finland); CEA and CNRS/IN2P3 (France); BMBF, DFG, and HGF (Germany); GSRI (Greece); NKFIH (Hungary); DAE and DST (India); IPM (Iran); SFI (Ireland); INFN (Italy); MSIP and NRF (Republic of Korea); MES (Latvia); LAS (Lithuania); MOE and UM (Malaysia); BUAP, CINVESTAV, CONACYT, LNS, SEP, and UASLP-FAI (Mexico); MOS (Montenegro); MBIE (New Zealand); PAEC

JHEP01(2024)128

(Pakistan); MES and NSC (Poland); FCT (Portugal); MESTD (Serbia); MCIN/AEI and PCTI (Spain); MOSTR (Sri Lanka); Swiss Funding Agencies (Switzerland); MST (Taipei); MHESI and NSTDA (Thailand); TUBITAK and TENMAK (Turkey); NASU (Ukraine); STFC (United Kingdom); DOE and NSF (U.S.A.).

Individuals have received support from the Marie-Curie program and the European Research Council and Horizon 2020 Grant, contract Nos. 675440, 724704, 752730, 758316, 765710, 824093, 884104, and COST Action CA16108 (European Union); the Leventis Foundation; the Alfred P. Sloan Foundation; the Alexander von Humboldt Foundation; the Science Committee, project no. 22rl-037 (Armenia); the Belgian Federal Science Policy Office; the Fonds pour la Formation à la Recherche dans l'Industrie et dans l'Agriculture (FRIA-Belgium); the Agentschap voor Innovatie door Wetenschap en Technologie (IWT-Belgium); the F.R.S.-FNRS and FWO (Belgium) under the "Excellence of Science — EOS" — be.h project n. 30820817; the Beijing Municipal Science & Technology Commission, No. Z191100007219010; the Ministry of Education, Youth and Sports (MEYS) of the Czech Republic; the Shota Rustaveli National Science Foundation, grant FR-22-985 (Georgia); the Deutsche Forschungsgemeinschaft (DFG), under Germany's Excellence Strategy — EXC 2121 "Quantum Universe" — 390833306, and under project number 400140256 — GRK2497; the Hellenic Foundation for Research and Innovation (HFRI), Project Number 2288 (Greece); the Hungarian Academy of Sciences, the New National Excellence Program — ÚNKP, the NKFIH research grants K 124845, K 124850, K 128713, K 128786, K 129058, K 131991, K 133046, K 138136, K 143460, K 143477, 2020-2.2.1-ED-2021-00181, and TKP2021-NKTA-64 (Hungary); the Council of Science and Industrial Research, India; the Latvian Council of Science; the Ministry of Education and Science, project no. 2022/WK/14, and the National Science Center, contracts Opus 2021/41/B/ST2/01369 and 2021/43/B/ST2/01552 (Poland); the Fundação para a Ciência e a Tecnologia, grant CEECIND/01334/2018 (Portugal); the National Priorities Research Program by Qatar National Research Fund; MCIN/AEI/10.13039/501100011033, ERDF "a way of making Europe", and the Programa Estatal de Fomento de la Investigación Científica y Técnica de Excelencia María de Maeztu, grant MDM-2017-0765 and Programa Severo Ochoa del Principado de Asturias (Spain); the Chulalongkorn Academic into Its 2nd Century Project Advancement Project, and the National Science, Research and Innovation Fund via the Program Management Unit for Human Resources & Institutional Development, Research and Innovation, grant B05F650021 (Thailand); the Kavli Foundation; the Nvidia Corporation; the SuperMicro Corporation; the Welch Foundation, contract C-1845; and the Weston Havens Foundation (U.S.A.).

JHEP01(2024)128

A Cross-experimental comparisons

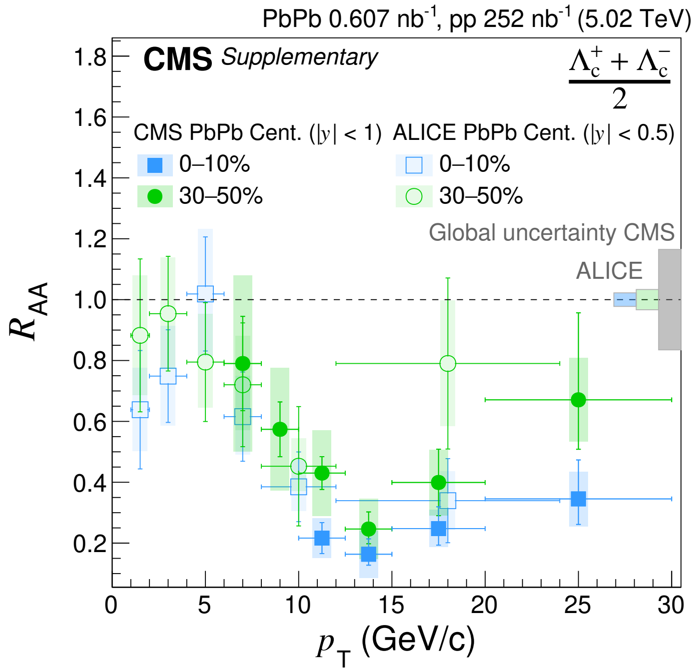

Figure 8. The nuclear modification factor R_{AA} vs. p_{T} for Λ_c^+ production in PbPb collisions. Results are shown for the 0–10 (closed squares) and 30–50% (closed circles) centrality ranges. Also shown are the published results from the ALICE Collaboration [27] for the same centrality ranges with open markers. The boxes and error bars represent the statistical and point-to-point systematic uncertainties, respectively. Global systematic uncertainties are indicated by the bands at unity. For CMS (gray band) this includes the uncertainties in the pp collision luminosity, the number of PbPb MB events, and the tracking efficiency. The global systematic uncertainties for the ALICE results (color bands) are shown separately for the two centrality ranges.

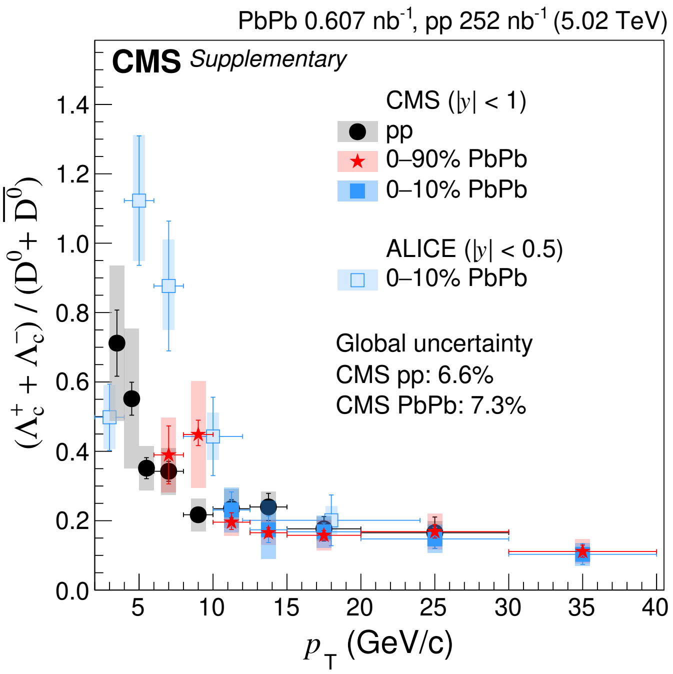

Figure 9. The ratio of the production cross sections of prompt Λ_c^+ to prompt D^0 versus p_T in pp collisions is represented by the closed circles. The ratio for the 0–90 (closed stars) and 0–10% (closed squares) centrality classes in PbPb collisions are compared to the pp result. The boxes and error bars represent the systematic and statistical uncertainties, respectively. The horizontal error bars represent the bin widths. The 6.6 and 7.3% normalization uncertainties in pp and PbPb collisions, respectively, are not included in the boxes representing the systematic uncertainties for each data point. Results from the ALICE Collaboration [27] for PbPb collisions in the 0–10% centrality class are also shown using the open square markers.

References

[1] E.V. Shuryak, *Theory of hadronic plasma*, *Sov. Phys. JETP* **47** (1978) 212 [INSPIRE].

[2] A. Andronic et al., *Heavy-flavour and quarkonium production in the LHC era: from proton-proton to heavy-ion collisions*, *Eur. Phys. J. C* **76** (2016) 107 [arXiv:1506.03981] [INSPIRE].

[3] F. Prino and R. Rapp, *Open heavy flavor in QCD matter and in nuclear collisions*, *J. Phys. G* **43** (2016) 093002 [arXiv:1603.00529] [INSPIRE].

[4] X. Dong and V. Greco, *Heavy quark production and properties of quark-gluon plasma*, *Prog. Part. Nucl. Phys.* **104** (2019) 97 [INSPIRE].

[5] X. Dong, Y.-J. Lee and R. Rapp, *Open heavy-flavor production in heavy-ion collisions*, *Ann. Rev. Nucl. Part. Sci.* **69** (2019) 417 [arXiv:1903.07709] [INSPIRE].

[6] W. Busza, K. Rajagopal and W. van der Schee, *Heavy ion collisions: the big picture, and the big questions*, *Ann. Rev. Nucl. Part. Sci.* **68** (2018) 339 [arXiv:1802.04801] [INSPIRE].

[7] L. Apolinário, Y.-J. Lee and M. Winn, *Heavy quarks and jets as probes of the QGP*, Prog. Part. Nucl. Phys. **127** (2022) 103990 [arXiv:2203.16352] [INSPIRE].

[8] A. Beraudo et al., *Extraction of heavy-flavor transport coefficients in QCD matter*, Nucl. Phys. A **979** (2018) 21 [arXiv:1803.03824] [INSPIRE].

[9] B. Andersson, G. Gustafson, G. Ingelman and T. Sjöstrand, *Parton fragmentation and string dynamics*, Phys. Rept. **97** (1983) 31 [INSPIRE].

[10] V. Greco, C.M. Ko and P. Levai, *Parton coalescence and anti-proton/pion anomaly at RHIC*, Phys. Rev. Lett. **90** (2003) 202302 [nucl-th/0301093] [INSPIRE].

[11] R.J. Fries, V. Greco and P. Sorensen, *Coalescence models for hadron formation from quark gluon plasma*, Ann. Rev. Nucl. Part. Sci. **58** (2008) 177 [arXiv:0807.4939] [INSPIRE].

[12] Y. Oh, C.M. Ko, S.H. Lee and S. Yasui, *Heavy baryon/meson ratios in relativistic heavy ion collisions*, Phys. Rev. C **79** (2009) 044905 [arXiv:0901.1382] [INSPIRE].

[13] S.H. Lee et al., *Λ_c enhancement from strongly coupled quark-gluon plasma*, Phys. Rev. Lett. **100** (2008) 222301 [arXiv:0709.3637] [INSPIRE].

[14] S. Ghosh et al., *Diffusion of Λ_c in hot hadronic medium and its impact on Λ_c/D ratio*, Phys. Rev. D **90** (2014) 054018 [arXiv:1407.5069] [INSPIRE].

[15] S. Plumari et al., *Charmed hadrons from coalescence plus fragmentation in relativistic nucleus-nucleus collisions at RHIC and LHC*, Eur. Phys. J. C **78** (2018) 348 [arXiv:1712.00730] [INSPIRE].

[16] ALICE collaboration, *Λ_c^+ production in pp collisions at $\sqrt{s} = 7$ TeV and in p-Pb collisions at $\sqrt{s_{\rm NN}} = 5.02$ TeV*, JHEP **04** (2018) 108 [arXiv:1712.09581] [INSPIRE].

[17] ALICE collaboration, *Λ_c^+ production and baryon-to-meson ratios in pp and p-Pb collisions at $\sqrt{s_{\rm NN}} = 5.02$ TeV at the LHC*, Phys. Rev. Lett. **127** (2021) 202301 [arXiv:2011.06078] [INSPIRE].

[18] CMS collaboration, *Production of Λ_c^+ baryons in proton-proton and lead-lead collisions at $\sqrt{s_{\rm NN}} = 5.02$ TeV*, Phys. Lett. B **803** (2020) 135328 [arXiv:1906.03322] [INSPIRE].

[19] LHCb collaboration, *Prompt charm production in pp collisions at $\sqrt{s} = 7$ TeV*, Nucl. Phys. B **871** (2013) 1 [arXiv:1302.2864] [INSPIRE].

[20] M.A.G. Aivazis, J.C. Collins, F.I. Olness and W.-K. Tung, *Leptoproduction of heavy quarks. 2. A unified QCD formulation of charged and neutral current processes from fixed target to collider energies*, Phys. Rev. D **50** (1994) 3102 [hep-ph/9312319] [INSPIRE].

[21] M. Benzke et al., *Prompt neutrinos from atmospheric charm in the general-mass variable-flavor-number scheme*, JHEP **12** (2017) 021 [arXiv:1705.10386] [INSPIRE].

[22] J.R. Christiansen and P.Z. Skands, *String formation beyond leading colour*, JHEP **08** (2015) 003 [arXiv:1505.01681] [INSPIRE].

[23] LHCb collaboration, *Prompt Λ_c^+ production in pPb collisions at $\sqrt{s_{\rm NN}} = 5.02$ TeV*, JHEP **02** (2019) 102 [arXiv:1809.01404] [INSPIRE].

[24] STAR collaboration, *First measurement of Λ_c baryon production in Au+Au collisions at $\sqrt{s_{\rm NN}} = 200$ GeV*, Phys. Rev. Lett. **124** (2020) 172301 [arXiv:1910.14628] [INSPIRE].

[25] T. Sjöstrand et al., *An introduction to PYTHIA 8.2*, Comput. Phys. Commun. **191** (2015) 159 [arXiv:1410.3012] [INSPIRE].

JHEP01(2024)128

[26] ALICE collaboration, *Λ_c^+ production in Pb-Pb collisions at $\sqrt{s_{NN}} = 5.02$ TeV*, Phys. Lett. B **793** (2019) 212 [arXiv:1809.10922] [INSPIRE].

[27] ALICE collaboration, *Constraining hadronization mechanisms with Λ_c^+/D^0 production ratios in Pb-Pb collisions at $\sqrt{s_{NN}} = 5.02$ TeV*, Phys. Lett. B **839** (2023) 137796 [arXiv:2112.08156] [INSPIRE].

[28] CMS collaboration, *Evidence for $X(3872)$ in Pb-Pb collisions and studies of its prompt production at $\sqrt{s_{NN}} = 5.02$ TeV*, Phys. Rev. Lett. **128** (2022) 032001 [arXiv:2102.13048] [INSPIRE].

[29] CMS collaboration, *Observation of the B_c^+ meson in Pb-Pb and pp collisions at $\sqrt{s_{NN}} = 5.02$ TeV and measurement of its nuclear modification factor*, Phys. Rev. Lett. **128** (2022) 252301 [arXiv:2201.02659] [INSPIRE].

[30] CMS collaboration, *CMS luminosity measurement using nucleus-nucleus collisions at $\sqrt{s_{_{NN}}} = 5.02$ TeV in 2018*, CMS-PAS-LUM-18-001, CERN, Geneva, Switzerland (2022).

[31] CMS collaboration, *Luminosity measurement in proton-proton collisions at 5.02 TeV in 2017 at CMS*, CMS-PAS-LUM-19-001, CERN, Geneva, Switzerland (2021).

[32] CMS collaboration, *Precision luminosity measurement in proton-proton collisions at $\sqrt{s} = 13$ TeV in 2015 and 2016 at CMS*, Eur. Phys. J. C **81** (2021) 800 [arXiv:2104.01927] [INSPIRE].

[33] M. He and R. Rapp, *Charm-baryon production in proton-proton collisions*, Phys. Lett. B **795** (2019) 117 [arXiv:1902.08889] [INSPIRE].

[34] CMS collaboration, *Nuclear modification factor of D^0 mesons in PbPb collisions at $\sqrt{s_{NN}} = 5.02$ TeV*, Phys. Lett. B **782** (2018) 474 [arXiv:1708.04962] [INSPIRE].

[35] *HEPData record for this analysis*, CMS-HIN-21-004, CERN, Geneva, Switzerland (2023) [DOI:10.17182/HEPDATA.135973].

[36] CMS collaboration, *Description and performance of track and primary-vertex reconstruction with the CMS tracker*, 2014 JINST **9** P10009 [arXiv:1405.6569] [INSPIRE].

[37] CMS collaboration, *The CMS experiment at the CERN LHC*, 2008 JINST **3** S08004 [INSPIRE].

[38] CMS collaboration, *Charged-particle nuclear modification factors in PbPb and pPb collisions at $\sqrt{s_{NN}} = 5.02$ TeV*, JHEP **04** (2017) 039 [arXiv:1611.01664] [INSPIRE].

[39] CMS collaboration, *Transverse momentum and pseudorapidity distributions of charged hadrons in pp collisions at $\sqrt{s} = 0.9$ and 2.36 TeV*, JHEP **02** (2010) 041 [arXiv:1002.0621] [INSPIRE].

[40] CMS collaboration, *The CMS trigger system*, 2017 JINST **12** P01020 [arXiv:1609.02366] [INSPIRE].

[41] CMS collaboration, *Event generator tunes obtained from underlying event and multiparton scattering measurements*, Eur. Phys. J. C **76** (2016) 155 [arXiv:1512.00815] [INSPIRE].

[42] I.P. Lokhtin and A.M. Snigirev, *A model of jet quenching in ultrarelativistic heavy ion collisions and high-p_T hadron spectra at RHIC*, Eur. Phys. J. C **45** (2006) 211 [hep-ph/0506189] [INSPIRE].

[43] D.J. Lange, *The EvtGen particle decay simulation package*, Nucl. Instrum. Meth. A **462** (2001) 152 [INSPIRE].

[44] Particle Data Group collaboration, *Review of particle physics*, PTEP **2022** (2022) 083C01 [INSPIRE].

JHEP01(2024)128

[45] GEANT4 collaboration, *GEANT4 — a simulation toolkit*, *Nucl. Instrum. Meth. A* **506** (2003) 250 [INSPIRE].

[46] E.L. Lehmann, *On likelihood ratio tests*, in *Optimality*, Institute of Mathematical Statistics (2006), p. 1 [DOI:10.1214/074921706000000356] [math/0610835].

[47] M. Cacciari, M. Greco and P. Nason, *The p_T spectrum in heavy-flavour hadroproduction*, *JHEP* **05** (1998) 007 [hep-ph/9803400] [INSPIRE].

[48] CMS collaboration, *Measurement of the total and differential inclusive B^+ hadron cross sections in pp collisions at $\sqrt{s} = 13$ TeV*, *Phys. Lett. B* **771** (2017) 435 [arXiv:1609.00873] [INSPIRE].

[49] M.L. Miller, K. Reygers, S.J. Sanders and P. Steinberg, *Glauber modeling in high energy nuclear collisions*, *Ann. Rev. Nucl. Part. Sci.* **57** (2007) 205 [nucl-ex/0701025] [INSPIRE].

[50] CMS collaboration, *Measurement of the $B^\pm$ meson nuclear modification factor in Pb-Pb collisions at $\sqrt{s_{\rm NN}} = 5.02$ TeV*, *Phys. Rev. Lett.* **119** (2017) 152301 [arXiv:1705.04727] [INSPIRE].

[51] B.A. Kniehl, G. Kramer, I. Schienbein and H. Spiesberger, *$\Lambda_c^\pm$ production in pp collisions with a new fragmentation function*, *Phys. Rev. D* **101** (2020) 114021 [arXiv:2004.04213] [INSPIRE].

[52] OPAL collaboration, *A study of charm hadron production in $Z^0 \to c\bar{c}$ and $Z^0 \to b\bar{b}$ decays at LEP*, *Z. Phys. C* **72** (1996) 1 [INSPIRE].

[53] BELLE collaboration, *Charm hadrons from fragmentation and B decays in e^+e^- annihilation at $\sqrt{s} = 10.6$ GeV*, *Phys. Rev. D* **73** (2006) 032002 [hep-ex/0506068] [INSPIRE].

[54] CMS collaboration, *Studies of beauty suppression via nonprompt D^0 mesons in Pb-Pb collisions at $Q^2 = 4$ GeV^2*, *Phys. Rev. Lett.* **123** (2019) 022001 [arXiv:1810.11102] [INSPIRE].

[55] V. Minissale, S. Plumari and V. Greco, *Charm hadrons in pp collisions at LHC energy within a coalescence plus fragmentation approach*, *Phys. Lett. B* **821** (2021) 136622 [arXiv:2012.12001] [INSPIRE].

[56] M. He and R. Rapp, *Hadronization and charm-hadron ratios in heavy-ion collisions*, *Phys. Rev. Lett.* **124** (2020) 042301 [arXiv:1905.09216] [INSPIRE].

The CMS collaboration

Yerevan Physics Institute, Yerevan, Armenia
A. Tumasyan[1]

Institut für Hochenergiephysik, Vienna, Austria
W. Adam, J.W. Andrejkovic, T. Bergauer, S. Chatterjee, K. Damanakis, M. Dragicevic, A. Escalante Del Valle, P.S. Hussain, M. Jeitler[2], N. Krammer, L. Lechner, D. Liko, I. Mikulec, P. Paulitsch, J. Schieck[2], R. Schöfbeck, D. Schwarz, M. Sonawane, S. Templ, W. Waltenberger, C.-E. Wulz[2]

Universiteit Antwerpen, Antwerpen, Belgium
M.R. Darwish[3], T. Janssen, T. Kello[4], P. Van Mechelen

Vrije Universiteit Brussel, Brussel, Belgium
E.S. Bols, J. D'Hondt, A. De Moor, M. Delcourt, H. El Faham, S. Lowette, A. Morton, D. Müller, A.R. Sahasransu, S. Tavernier, W. Van Doninck, S. Van Putte, D. Vannerom

Université Libre de Bruxelles, Bruxelles, Belgium
B. Clerbaux, S. Dansana, G. De Lentdecker, L. Favart, D. Hohov, J. Jaramillo, K. Lee, M. Mahdavikhorrami, I. Makarenko, A. Malara, S. Paredes, L. Pétré, N. Postiau, L. Thomas, M. Vanden Bemden, C. Vander Velde, P. Vanlaer

Ghent University, Ghent, Belgium
D. Dobur, J. Knolle, L. Lambrecht, G. Mestdach, C. Rendón, A. Samalan, K. Skovpen, M. Tytgat, N. Van Den Bossche, B. Vermassen, L. Wezenbeek

Université Catholique de Louvain, Louvain-la-Neuve, Belgium
A. Benecke, G. Bruno, F. Bury, C. Caputo, P. David, C. Delaere, I.S. Donertas, A. Giammanco, K. Jaffel, Sa. Jain, V. Lemaitre, K. Mondal, A. Taliercio, T.T. Tran, P. Vischia, S. Wertz

Centro Brasileiro de Pesquisas Fisicas, Rio de Janeiro, Brazil
G.A. Alves, E. Coelho, C. Hensel, A. Moraes, P. Rebello Teles

Universidade do Estado do Rio de Janeiro, Rio de Janeiro, Brazil
W.L. Aldá Júnior, M. Alves Gallo Pereira, M. Barroso Ferreira Filho, H. Brandao Malbouisson, W. Carvalho, J. Chinellato[5], E.M. Da Costa, G.G. Da Silveira[6], D. De Jesus Damiao, V. Dos Santos Sousa, S. Fonseca De Souza, J. Martins[7], C. Mora Herrera, K. Mota Amarilo, L. Mundim, H. Nogima, A. Santoro, S.M. Silva Do Amaral, A. Sznajder, M. Thiel, A. Vilela Pereira

Universidade Estadual Paulista, Universidade Federal do ABC, São Paulo, Brazil
C.A. Bernardes[6], L. Calligaris, T.R. Fernandez Perez Tomei, E.M. Gregores, P.G. Mercadante, S.F. Novaes, Sandra S. Padula

JHEP01(2024)128

Institute for Nuclear Research and Nuclear Energy, Bulgarian Academy of Sciences, Sofia, Bulgaria
A. Aleksandrov, G. Antchev, R. Hadjiiska, P. Iaydjiev, M. Misheva, M. Rodozov, M. Shopova, G. Sultanov

University of Sofia, Sofia, Bulgaria
A. Dimitrov, T. Ivanov, L. Litov, B. Pavlov, P. Petkov, A. Petrov, E. Shumka

Instituto De Alta Investigación, Universidad de Tarapacá, Casilla 7 D, Arica, Chile
S. Keshri, S. Thakur

Beihang University, Beijing, China
T. Cheng, Q. Guo, T. Javaid[8], M. Mittal, L. Yuan

Department of Physics, Tsinghua University, Beijing, China
G. Bauer[9], Z. Hu, S. Lezki, K. Yi[9,10]

Institute of High Energy Physics, Beijing, China
G.M. Chen[8], H.S. Chen[8], M. Chen[8], F. Iemmi, C.H. Jiang, A. Kapoor, H. Liao, Z.-A. Liu[11], V. Milosevic, F. Monti, R. Sharma, J. Tao, J. Thomas-Wilsker, J. Wang, H. Zhang, J. Zhao

State Key Laboratory of Nuclear Physics and Technology, Peking University, Beijing, China
A. Agapitos, Y. Ban, A. Carvalho Antunes De Oliveira, A. Levin, C. Li, Q. Li, X. Lyu, Y. Mao, S.J. Qian, X. Sun, D. Wang, J. Xiao, H. Yang

Sun Yat-Sen University, Guangzhou, China
M. Lu, Z. You

University of Science and Technology of China, Hefei, China
N. Lu

Institute of Modern Physics and Key Laboratory of Nuclear Physics and Ion-beam Application (MOE) — Fudan University, Shanghai, China
X. Gao[4], D. Leggat, H. Okawa, Y. Zhang

Zhejiang University, Hangzhou, Zhejiang, China
Z. Lin, C. Lu, M. Xiao

Universidad de Los Andes, Bogota, Colombia
C. Avila, D.A. Barbosa Trujillo, A. Cabrera, C. Florez, J. Fraga

Universidad de Antioquia, Medellin, Colombia
J. Mejia Guisao, F. Ramirez, M. Rodriguez, J.D. Ruiz Alvarez

JHEP01(2024)128

University of Split, Faculty of Electrical Engineering, Mechanical Engineering and Naval Architecture, Split, Croatia
D. Giljanovic, N. Godinovic, D. Lelas, I. Puljak

University of Split, Faculty of Science, Split, Croatia
Z. Antunovic, M. Kovac, T. Sculac

Institute Rudjer Boskovic, Zagreb, Croatia
P. Bargassa, V. Brigljevic, B.K. Chitroda, D. Ferencek, S. Mishra, M. Roguljic, A. Starodumov[12], T. Susa

University of Cyprus, Nicosia, Cyprus
A. Attikis, K. Christoforou, S. Konstantinou, J. Mousa, C. Nicolaou, F. Ptochos, P.A. Razis, H. Rykaczewski, H. Saka, A. Stepennov

Charles University, Prague, Czech Republic
M. Finger, M. Finger Jr., A. Kveton

Escuela Politecnica Nacional, Quito, Ecuador
E. Ayala

Universidad San Francisco de Quito, Quito, Ecuador
E. Carrera Jarrin

Academy of Scientific Research and Technology of the Arab Republic of Egypt, Egyptian Network of High Energy Physics, Cairo, Egypt
Y. Assran[13,14], S. Elgammal[14]

Center for High Energy Physics (CHEP-FU), Fayoum University, El-Fayoum, Egypt
M. Abdullah Al-Mashad, M.A. Mahmoud

National Institute of Chemical Physics and Biophysics, Tallinn, Estonia
S. Bhowmik, R.K. Dewanjee, K. Ehataht, M. Kadastik, T. Lange, S. Nandan, C. Nielsen, J. Pata, M. Raidal, L. Tani, C. Veelken

Department of Physics, University of Helsinki, Helsinki, Finland
P. Eerola, H. Kirschenmann, K. Osterberg, M. Voutilainen

Helsinki Institute of Physics, Helsinki, Finland
S. Bharthuar, E. Brücken, F. Garcia, J. Havukainen, M.S. Kim, R. Kinnunen, T. Lampén, K. Lassila-Perini, S. Lehti, T. Lindén, M. Lotti, L. Martikainen, M. Myllymäki, M.m. Rantanen, H. Siikonen, E. Tuominen, J. Tuominiemi

Lappeenranta-Lahti University of Technology, Lappeenranta, Finland
P. Luukka, H. Petrow, T. Tuuva[†]

JHEP01(2024)128

IRFU, CEA, Université Paris-Saclay, Gif-sur-Yvette, France
C. Amendola, M. Besancon, F. Couderc, M. Dejardin, D. Denegri, J.L. Faure, F. Ferri, S. Ganjour, P. Gras, G. Hamel de Monchenault, V. Lohezic, J. Malcles, J. Rander, A. Rosowsky, M.Ö. Sahin, A. Savoy-Navarro[15], P. Simkina, M. Titov

Laboratoire Leprince-Ringuet, CNRS/IN2P3, Ecole Polytechnique, Institut Polytechnique de Paris, Palaiseau, France
C. Baldenegro Barrera, F. Beaudette, A. Buchot Perraguin, P. Busson, A. Cappati, C. Charlot, F. Damas, O. Davignon, B. Diab, G. Falmagne, B.A. Fontana Santos Alves, S. Ghosh, R. Granier de Cassagnac, A. Hakimi, B. Harikrishnan, G. Liu, J. Motta, M. Nguyen, C. Ochando, L. Portales, R. Salerno, U. Sarkar, J.B. Sauvan, Y. Sirois, A. Tarabini, E. Vernazza, A. Zabi, A. Zghiche

Université de Strasbourg, CNRS, IPHC UMR 7178, Strasbourg, France
J.-L. Agram[16], J. Andrea, D. Apparu, D. Bloch, G. Bourgatte, J.-M. Brom, E.C. Chabert, C. Collard, D. Darej, U. Goerlach, C. Grimault, A.-C. Le Bihan, P. Van Hove

Institut de Physique des 2 Infinis de Lyon (IP2I), Villeurbanne, France
S. Beauceron, B. Blancon, G. Boudoul, A. Carle, N. Chanon, J. Choi, D. Contardo, P. Depasse, C. Dozen[17], H. El Mamouni, J. Fay, S. Gascon, M. Gouzevitch, G. Grenier, B. Ille, I.B. Laktineh, M. Lethuillier, L. Mirabito, S. Perries, M. Vander Donckt, P. Verdier, S. Viret

Georgian Technical University, Tbilisi, Georgia
D. Lomidze, I. Lomidze, Z. Tsamalaidze[12]

RWTH Aachen University, I. Physikalisches Institut, Aachen, Germany
V. Botta, L. Feld, K. Klein, M. Lipinski, D. Meuser, A. Pauls, N. Röwert, M. Teroerde

RWTH Aachen University, III. Physikalisches Institut A, Aachen, Germany
S. Diekmann, A. Dodonova, N. Eich, D. Eliseev, M. Erdmann, P. Fackeldey, B. Fischer, T. Hebbeker, K. Hoepfner, F. Ivone, M.y. Lee, L. Mastrolorenzo, M. Merschmeyer, A. Meyer, S. Mondal, S. Mukherjee, D. Noll, A. Novak, F. Nowotny, A. Pozdnyakov, Y. Rath, W. Redjeb, F. Rehm, H. Reithler, A. Schmidt, S.C. Schuler, A. Sharma, A. Stein, F. Torres Da Silva De Araujo[18], L. Vigilante, S. Wiedenbeck, S. Zaleski

RWTH Aachen University, III. Physikalisches Institut B, Aachen, Germany
C. Dziwok, G. Flügge, W. Haj Ahmad[19], O. Hlushchenko, T. Kress, A. Nowack, O. Pooth, A. Stahl, T. Ziemons, A. Zotz

Deutsches Elektronen-Synchrotron, Hamburg, Germany
H. Aarup Petersen, M. Aldaya Martin, J. Alimena, Y. An, P. Asmuss, S. Baxter, M. Bayatmakou, H. Becerril Gonzalez, O. Behnke, S. Bhattacharya, F. Blekman[20], K. Borras[21], D. Brunner, A. Campbell, A. Cardini, C. Cheng, F. Colombina,

S. Consuegra Rodríguez, G. Correia Silva, M. De Silva, G. Eckerlin, D. Eckstein, L.I. Estevez Banos, O. Filatov, E. Gallo[20], A. Geiser, A. Giraldi, G. Greau, A. Grohsjean, V. Guglielmi, M. Guthoff, A. Jafari[22], N.Z. Jomhari, B. Kaech, M. Kasemann, H. Kaveh, C. Kleinwort, R. Kogler, M. Komm, D. Krücker, W. Lange, D. Leyva Pernia, K. Lipka[23], W. Lohmann[24], R. Mankel, I.-A. Melzer-Pellmann, M. Mendizabal Morentin, J. Metwally, A.B. Meyer, G. Milella, M. Mormile, A. Mussgiller, A. Nürnberg, Y. Otarid, D. Pérez Adán, E. Ranken, A. Raspereza, B. Ribeiro Lopes, J. Rübenach, A. Saggio, M. Savitskyi, M. Scham[25,21], V. Scheurer, S. Schnake[21], P. Schütze, C. Schwanenberger[20], M. Shchedrolosiev, R.E. Sosa Ricardo, D. Stafford, N. Tonon[†], F. Vazzoler, A. Ventura Barroso, R. Walsh, Q. Wang, Y. Wen, K. Wichmann, L. Wiens[21], C. Wissing, S. Wuchterl, Y. Yang, A. Zimermmane Castro Santos

University of Hamburg, Hamburg, Germany

A. Albrecht, S. Albrecht, M. Antonello, S. Bein, L. Benato, M. Bonanomi, P. Connor, K. De Leo, M. Eich, K. El Morabit, A. Fröhlich, C. Garbers, E. Garutti, M. Hajheidari, J. Haller, A. Hinzmann, H.R. Jabusch, G. Kasieczka, P. Keicher, R. Klanner, W. Korcari, T. Kramer, V. Kutzner, F. Labe, J. Lange, A. Lobanov, C. Matthies, A. Mehta, L. Moureaux, M. Mrowietz, A. Nigamova, Y. Nissan, A. Paasch, K.J. Pena Rodriguez, T. Quadfasel, M. Rieger, D. Savoiu, J. Schindler, P. Schleper, M. Schröder, J. Schwandt, M. Sommerhalder, H. Stadie, G. Steinbrück, A. Tews, M. Wolf

Karlsruher Institut fuer Technologie, Karlsruhe, Germany

S. Brommer, M. Burkart, E. Butz, T. Chwalek, A. Dierlamm, A. Droll, N. Faltermann, M. Giffels, J.O. Gosewisch, A. Gottmann, F. Hartmann[26], M. Horzela, U. Husemann, M. Klute, R. Koppenhöfer, M. Link, A. Lintuluoto, S. Maier, S. Mitra, Th. Müller, M. Neukum, M. Oh, G. Quast, K. Rabbertz, I. Shvetsov, H.J. Simonis, N. Trevisani, R. Ulrich, J. van der Linden, R.F. Von Cube, M. Wassmer, S. Wieland, R. Wolf, S. Wunsch, X. Zuo

Institute of Nuclear and Particle Physics (INPP), NCSR Demokritos, Aghia Paraskevi, Greece

G. Anagnostou, P. Assiouras, G. Daskalakis, A. Kyriakis, A. Stakia

National and Kapodistrian University of Athens, Athens, Greece

M. Diamantopoulou, D. Karasavvas, P. Kontaxakis, A. Manousakis-Katsikakis, G. Melachroinos, A. Panagiotou, I. Papavergou, N. Saoulidou, K. Theofilatos, E. Tziaferi, K. Vellidis, I. Zisopoulos

National Technical University of Athens, Athens, Greece

G. Bakas, T. Chatzistavrou, G. Karapostoli, K. Kousouris, I. Papakrivopoulos, G. Tsipolitis, A. Zacharopoulou

JHEP01(2024)128

University of Ioánnina, Ioánnina, Greece
K. Adamidis, I. Bestintzanos, I. Evangelou, C. Foudas, P. Gianneios, C. Kamtsikis, P. Katsoulis, P. Kokkas, P.G. Kosmoglou Kioseoglou, N. Manthos, I. Papadopoulos, J. Strologas

MTA-ELTE Lendület CMS Particle and Nuclear Physics Group, Eötvös Loránd University, Budapest, Hungary
M. Csanád, K. Farkas, M.M.A. Gadallah[27], P. Major, K. Mandal, G. Pásztor, A.J. Rádl[28], O. Surányi, G.I. Veres

Wigner Research Centre for Physics, Budapest, Hungary
M. Bartók[29], C. Hajdu, D. Horvath[30,31], F. Sikler, V. Veszpremi

Institute of Nuclear Research ATOMKI, Debrecen, Hungary
G. Bencze, N. Beni, S. Czellar, J. Karancsi[29], J. Molnar, Z. Szillasi, D. Teyssier

Institute of Physics, University of Debrecen, Debrecen, Hungary
P. Raics, B. Ujvari[32], G. Zilizi

Karoly Robert Campus, MATE Institute of Technology, Gyongyos, Hungary
T. Csorgo[28], F. Nemes[28], T. Novak

Panjab University, Chandigarh, India
J. Babbar, S. Bansal, S.B. Beri, V. Bhatnagar, G. Chaudhary, S. Chauhan, N. Dhingra[33], R. Gupta, A. Kaur, A. Kaur, H. Kaur, M. Kaur, S. Kumar, P. Kumari, M. Meena, K. Sandeep, T. Sheokand, J.B. Singh[34], A. Singla

University of Delhi, Delhi, India
A. Ahmed, A. Bhardwaj, A. Chhetri, B.C. Choudhary, A. Kumar, M. Naimuddin, K. Ranjan, S. Saumya

Saha Institute of Nuclear Physics, HBNI, Kolkata, India
S. Baradia, S. Barman[35], S. Bhattacharya, D. Bhowmik, S. Dutta, S. Dutta, B. Gomber[36], M. Maity[35], P. Palit, G. Saha, B. Sahu[36], S. Sarkar

Indian Institute of Technology Madras, Madras, India
P.K. Behera, S.C. Behera, S. Chatterjee, P. Kalbhor, J.R. Komaragiri[37], D. Kumar[37], A. Muhammad, L. Panwar[37], R. Pradhan, P.R. Pujahari, N.R. Saha, A. Sharma, A.K. Sikdar, S. Verma

Bhabha Atomic Research Centre, Mumbai, India
K. Naskar[38]

Tata Institute of Fundamental Research-A, Mumbai, India
T. Aziz, I. Das, S. Dugad, M. Kumar, G.B. Mohanty, P. Suryadevara

Tata Institute of Fundamental Research-B, Mumbai, India
S. Banerjee, M. Guchait, S. Karmakar, S. Kumar, G. Majumder, K. Mazumdar, S. Mukherjee, A. Thachayath

JHEP01(2024)128

National Institute of Science Education and Research, An OCC of Homi Bhabha National Institute, Bhubaneswar, Odisha, India
S. Bahinipati[39], A.K. Das, C. Kar, P. Mal, T. Mishra, V.K. Muraleedharan Nair Bindhu[40], A. Nayak[40], P. Saha, S.K. Swain, S. Varghese, D. Vats[40]

Indian Institute of Science Education and Research (IISER), Pune, India
A. Alpana, S. Dube, B. Kansal, A. Laha, S. Pandey, A. Rastogi, S. Sharma

Isfahan University of Technology, Isfahan, Iran
H. Bakhshiansohi[41,42], E. Khazaie[42], M. Zeinali[43]

Institute for Research in Fundamental Sciences (IPM), Tehran, Iran
S. Chenarani[44], S.M. Etesami, M. Khakzad, M. Mohammadi Najafabadi

University College Dublin, Dublin, Ireland
M. Grunewald

INFN Sezione di Bari[a], Università di Bari[b], Politecnico di Bari[c], Bari, Italy
M. Abbrescia[a,b], R. Aly[a,b,45], C. Aruta[a,b], A. Colaleo[a], D. Creanza[a,c], L. Cristella[a,b], B. D' Anzi[a,b], N. De Filippis[a,c], M. De Palma[a,b], A. Di Florio[a,b], W. Elmetenawee[a,b], F. Errico[a,b], L. Fiore[a], G. Iaselli[a,c], G. Maggi[a,c], M. Maggi[a], I. Margjeka[a,b], V. Mastrapasqua[a,b], S. My[a,b], S. Nuzzo[a,b], A. Pellecchia[a,b], A. Pompili[a,b], G. Pugliese[a,c], R. Radogna[a], D. Ramos[a], A. Ranieri[a], G. Selvaggi[a,b], L. Silvestris[a], F.M. Simone[a,b], Ü. Sözbilir[a], A. Stamerra[a], R. Venditti[a], P. Verwilligen[a]

INFN Sezione di Bologna[a], Università di Bologna[b], Bologna, Italy
G. Abbiendi[a], C. Battilana[a,b], D. Bonacorsi[a,b], L. Borgonovi[a], L. Brigliadori[a], R. Campanini[a,b], P. Capiluppi[a,b], A. Castro[a,b], F.R. Cavallo[a], M. Cuffiani[a,b], G.M. Dallavalle[a], T. Diotalevi[a,b], F. Fabbri[a], A. Fanfani[a,b], D. Fasanella[a,b], P. Giacomelli[a], L. Giommi[a,b], C. Grandi[a], L. Guiducci[a,b], S. Lo Meo[a,46], L. Lunerti[a,b], S. Marcellini[a], G. Masetti[a], F.L. Navarria[a,b], A. Perrotta[a], F. Primavera[a,b], A.M. Rossi[a,b], T. Rovelli[a,b], G.P. Siroli[a,b]

INFN Sezione di Catania[a], Università di Catania[b], Catania, Italy
S. Costa[a,b,47], A. Di Mattia[a], R. Potenza[a,b], A. Tricomi[a,b,47], C. Tuve[a,b]

INFN Sezione di Firenze[a], Università di Firenze[b], Firenze, Italy
G. Barbagli[a], G. Bardelli[a,b], B. Camaiani[a,b], A. Cassese[a], R. Ceccarelli[a,b], V. Ciulli[a,b], C. Civinini[a], R. D'Alessandro[a,b], E. Focardi[a,b], G. Latino[a,b], P. Lenzi[a,b], M. Lizzo[a,b], M. Meschini[a], S. Paoletti[a], G. Sguazzoni[a], L. Viliani[a]

INFN Laboratori Nazionali di Frascati, Frascati, Italy
L. Benussi, S. Bianco, S. Meola[48], D. Piccolo

INFN Sezione di Genova[a], Università di Genova[b], Genova, Italy
M. Bozzo[a,b], P. Chatagnon[a], F. Ferro[a], E. Robutti[a], S. Tosi[a,b]

JHEP01(2024)128

INFN Sezione di Milano-Bicocca[a], Università di Milano-Bicocca[b], Milano, Italy

A. Benaglia[a], G. Boldrini[a], F. Brivio[a,b], F. Cetorelli[a,b], F. De Guio[a,b], M.E. Dinardo[a,b], P. Dini[a], S. Gennai[a], A. Ghezzi[a,b], P. Govoni[a,b], L. Guzzi[a,b], M.T. Lucchini[a,b], M. Malberti[a], S. Malvezzi[a], A. Massironi[a], D. Menasce[a], L. Moroni[a], M. Paganoni[a,b], D. Pedrini[a], B.S. Pinolini[a], S. Ragazzi[a,b], N. Redaelli[a], T. Tabarelli de Fatis[a,b], D. Zuolo[a,b]

INFN Sezione di Napoli[a], Università di Napoli 'Federico II'[b], Napoli, Italy; Università della Basilicata[c], Potenza, Italy; Università G. Marconi[d], Roma, Italy

S. Buontempo[a], A. Cagnotta[a,b], F. Carnevali[a,b], N. Cavallo[a,c], A. De Iorio[a,b], F. Fabozzi[a,c], A.O.M. Iorio[a,b], L. Lista[a,b,49], P. Paolucci[a,26], B. Rossi[a], C. Sciacca[a,b]

INFN Sezione di Padova[a], Università di Padova[b], Padova, Italy; Università di Trento[c], Trento, Italy

R. Ardino[a], P. Azzi[a], N. Bacchetta[a,50], M. Benettoni[a], A. Bergnoli[a], P. Bortignon[a], A. Bragagnolo[a,b], R. Carlin[a,b], P. Checchia[a], T. Dorigo[a], U. Gasparini[a,b], G. Grosso[a], L. Layer[a,51], E. Lusiani[a], M. Margoni[a,b], A.T. Meneguzzo[a,b], J. Pazzini[a,b], P. Ronchese[a,b], R. Rossin[a,b], F. Simonetto[a,b], G. Strong[a], M. Tosi[a,b], H. Yarar[a,b], M. Zanetti[a,b], P. Zotto[a,b], A. Zucchetta[a,b], G. Zumerle[a,b]

INFN Sezione di Pavia[a], Università di Pavia[b], Pavia, Italy

S. Abu Zeid[a,52], C. Aimè[a,b], A. Braghieri[a], S. Calzaferri[a,b], D. Fiorina[a,b], P. Montagna[a,b], V. Re[a], C. Riccardi[a,b], P. Salvini[a], I. Vai[a,b], P. Vitulo[a,b]

INFN Sezione di Perugia[a], Università di Perugia[b], Perugia, Italy

P. Asenov[a,53], G.M. Bilei[a], D. Ciangottini[a,b], L. Fanò[a,b], M. Magherini[a,b], G. Mantovani[a,b], V. Mariani[a,b], M. Menichelli[a], F. Moscatelli[a,53], A. Piccinelli[a,b], M. Presilla[a,b], A. Rossi[a,b], A. Santocchia[a,b], D. Spiga[a], T. Tedeschi[a,b]

INFN Sezione di Pisa[a], Università di Pisa[b], Scuola Normale Superiore di Pisa[c], Pisa, Italy; Università di Siena[d], Siena, Italy

P. Azzurri[a], G. Bagliesi[a], V. Bertacchi[a,c], R. Bhattacharya[a], L. Bianchini[a,b], T. Boccali[a], E. Bossini[a,b], D. Bruschini[a,c], R. Castaldi[a], M.A. Ciocci[a,b], V. D'Amante[a,d], R. Dell'Orso[a], S. Donato[a], A. Giassi[a], F. Ligabue[a,c], D. Matos Figueiredo[a], A. Messineo[a,b], M. Musich[a,b], F. Palla[a], S. Parolia[a], G. Ramirez-Sanchez[a,c], A. Rizzi[a,b], G. Rolandi[a,c], S. Roy Chowdhury[a], T. Sarkar[a], A. Scribano[a], P. Spagnolo[a], R. Tenchini[a], G. Tonelli[a,b], N. Turini[a,d], A. Venturi[a], P.G. Verdini[a]

INFN Sezione di Roma[a], Sapienza Università di Roma[b], Roma, Italy

P. Barria[a], M. Campana[a,b], F. Cavallari[a], D. Del Re[a,b], E. Di Marco[a], M. Diemoz[a], E. Longo[a,b], P. Meridiani[a], G. Organtini[a,b], F. Pandolfi[a], R. Paramatti[a,b], C. Quaranta[a,b], S. Rahatlou[a,b], C. Rovelli[a], F. Santanastasio[a,b], L. Soffi[a], R. Tramontano[a,b]

JHEP01(2024)128

INFN Sezione di Torino[a], Università di Torino[b], Torino, Italy; Università del Piemonte Orientale[c], Novara, Italy

N. Amapane[a,b], R. Arcidiacono[a,c], S. Argiro[a,b], M. Arneodo[a,c], N. Bartosik[a], R. Bellan[a,b], A. Bellora[a,b], C. Biino[a], N. Cartiglia[a], M. Costa[a,b], R. Covarelli[a,b], N. Demaria[a], L. Finco[a], M. Grippo[a,b], B. Kiani[a,b], F. Legger[a], F. Luongo[a,b], C. Mariotti[a], S. Maselli[a], A. Mecca[a,b], E. Migliore[a,b], M. Monteno[a], R. Mulargia[a], M.M. Obertino[a,b], G. Ortona[a], L. Pacher[a,b], N. Pastrone[a], M. Pelliccioni[a], M. Ruspa[a,c], K. Shchelina[a], F. Siviero[a,b], V. Sola[a,b], A. Solano[a,b], D. Soldi[a,b], A. Staiano[a], C. Tarricone[a,b], M. Tornago[a,b], D. Trocino[a], G. Umoret[a,b], A. Vagnerini[a,b], E. Vlasov[a,b]

INFN Sezione di Trieste[a], Università di Trieste[b], Trieste, Italy

S. Belforte[a], V. Candelise[a,b], M. Casarsa[a], F. Cossutti[a], G. Della Ricca[a,b], G. Sorrentino[a,b]

Kyungpook National University, Daegu, Korea

S. Dogra, C. Huh, B. Kim, D.H. Kim, G.N. Kim, J. Kim, J. Lee, S.W. Lee, C.S. Moon, Y.D. Oh, S.I. Pak, M.S. Ryu, S. Sekmen, Y.C. Yang

Chonnam National University, Institute for Universe and Elementary Particles, Kwangju, Korea

H. Kim, D.H. Moon

Hanyang University, Seoul, Korea

E. Asilar, T.J. Kim, J. Park

Korea University, Seoul, Korea

S. Choi, S. Han, B. Hong, K. Lee, K.S. Lee, J. Lim, J. Park, S.K. Park, J. Yoo

Kyung Hee University, Department of Physics, Seoul, Korea

J. Goh

Sejong University, Seoul, Korea

H. S. Kim, Y. Kim, S. Lee

Seoul National University, Seoul, Korea

J. Almond, J.H. Bhyun, J. Choi, S. Jeon, J. Kim, J.S. Kim, S. Ko, H. Kwon, H. Lee, S. Lee, B.H. Oh, S.B. Oh, H. Seo, U.K. Yang, I. Yoon

University of Seoul, Seoul, Korea

W. Jang, D.Y. Kang, Y. Kang, D. Kim, S. Kim, B. Ko, J.S.H. Lee, Y. Lee, J.A. Merlin, I.C. Park, Y. Roh, D. Song, I.J. Watson, S. Yang

Yonsei University, Department of Physics, Seoul, Korea

S. Ha, H.D. Yoo

Sungkyunkwan University, Suwon, Korea

M. Choi, M.R. Kim, H. Lee, Y. Lee, I. Yu

JHEP01(2024)128

College of Engineering and Technology, American University of the Middle East (AUM), Dasman, Kuwait
T. Beyrouthy, Y. Maghrbi

Riga Technical University, Riga, Latvia
K. Dreimanis, G. Pikurs, A. Potrebko, M. Seidel, V. Veckalns[54]

Vilnius University, Vilnius, Lithuania
M. Ambrozas, A. Juodagalvis, A. Rinkevicius, G. Tamulaitis

National Centre for Particle Physics, Universiti Malaya, Kuala Lumpur, Malaysia
N. Bin Norjoharuddeen, S.Y. Hoh[55], I. Yusuff[55], Z. Zolkapli

Universidad de Sonora (UNISON), Hermosillo, Mexico
J.F. Benitez, A. Castaneda Hernandez, H.A. Encinas Acosta, L.G. Gallegos Maríñez, M. León Coello, J.A. Murillo Quijada, A. Sehrawat, L. Valencia Palomo

Centro de Investigacion y de Estudios Avanzados del IPN, Mexico City, Mexico
G. Ayala, H. Castilla-Valdez, I. Heredia-De La Cruz[56], R. Lopez-Fernandez, C.A. Mondragon Herrera, D.A. Perez Navarro, A. Sánchez Hernández

Universidad Iberoamericana, Mexico City, Mexico
C. Oropeza Barrera, F. Vazquez Valencia

Benemerita Universidad Autonoma de Puebla, Puebla, Mexico
I. Pedraza, H.A. Salazar Ibarguen, C. Uribe Estrada

University of Montenegro, Podgorica, Montenegro
I. Bubanja, J. Mijuskovic[57], N. Raicevic

National Centre for Physics, Quaid-I-Azam University, Islamabad, Pakistan
A. Ahmad, M.I. Asghar, A. Awais, M.I.M. Awan, M. Gul, H.R. Hoorani, W.A. Khan

AGH University of Science and Technology Faculty of Computer Science, Electronics and Telecommunications, Krakow, Poland
V. Avati, L. Grzanka, M. Malawski

National Centre for Nuclear Research, Swierk, Poland
H. Bialkowska, M. Bluj, B. Boimska, M. Górski, M. Kazana, M. Szleper, P. Zalewski

Institute of Experimental Physics, Faculty of Physics, University of Warsaw, Warsaw, Poland
K. Bunkowski, K. Doroba, A. Kalinowski, M. Konecki, J. Krolikowski

JHEP01(2024)128

Laboratório de Instrumentação e Física Experimental de Partículas, Lisboa, Portugal
M. Araujo, D. Bastos, A. Boletti, P. Faccioli, M. Gallinaro, J. Hollar, N. Leonardo, T. Niknejad, M. Pisano, J. Seixas, J. Varela

Faculty of Physics, University of Belgrade, Belgrade, Serbia
P. Adzic[58], P. Milenovic

VINCA Institute of Nuclear Sciences, University of Belgrade, Belgrade, Serbia
M. Dordevic, J. Milosevic

Centro de Investigaciones Energéticas Medioambientales y Tecnológicas (CIEMAT), Madrid, Spain
M. Aguilar-Benitez, J. Alcaraz Maestre, M. Barrio Luna, Cristina F. Bedoya, M. Cepeda, M. Cerrada, N. Colino, B. De La Cruz, A. Delgado Peris, D. Fernández Del Val, J.P. Fernández Ramos, J. Flix, M.C. Fouz, O. Gonzalez Lopez, S. Goy Lopez, J.M. Hernandez, M.I. Josa, J. León Holgado, D. Moran, C. Perez Dengra, A. Pérez-Calero Yzquierdo, J. Puerta Pelayo, I. Redondo, D.D. Redondo Ferrero, L. Romero, S. Sánchez Navas, J. Sastre, L. Urda Gómez, J. Vazquez Escobar, C. Willmott

Universidad Autónoma de Madrid, Madrid, Spain
J.F. de Trocóniz

Universidad de Oviedo, Instituto Universitario de Ciencias y Tecnologías Espaciales de Asturias (ICTEA), Oviedo, Spain
B. Alvarez Gonzalez, J. Cuevas, J. Fernandez Menendez, S. Folgueras, I. Gonzalez Caballero, J.R. González Fernández, E. Palencia Cortezon, C. Ramón Álvarez, V. Rodríguez Bouza, A. Soto Rodríguez, A. Trapote, C. Vico Villalba

Instituto de Física de Cantabria (IFCA), CSIC-Universidad de Cantabria, Santander, Spain
J.A. Brochero Cifuentes, I.J. Cabrillo, A. Calderon, J. Duarte Campderros, M. Fernandez, C. Fernandez Madrazo, G. Gomez, C. Lasaosa García, C. Martinez Rivero, P. Martinez Ruiz del Arbol, F. Matorras, P. Matorras Cuevas, J. Piedra Gomez, C. Prieels, L. Scodellaro, I. Vila, J.M. Vizan Garcia

University of Colombo, Colombo, Sri Lanka
M.K. Jayananda, B. Kailasapathy[59], D.U.J. Sonnadara, D.D.C. Wickramarathna

University of Ruhuna, Department of Physics, Matara, Sri Lanka
W.G.D. Dharmaratna, K. Liyanage, N. Perera, N. Wickramage

CERN, European Organization for Nuclear Research, Geneva, Switzerland
D. Abbaneo, E. Auffray, G. Auzinger, J. Baechler, P. Baillon[†], D. Barney, A. Bermúdez Martínez, M. Bianco, B. Bilin, A.A. Bin Anuar, A. Bocci, E. Brondolin, C. Caillol, T. Camporesi, G. Cerminara, N. Chernyavskaya, S.S. Chhibra, S. Choudhury,

M. Cipriani, D. d'Enterria, A. Dabrowski, A. David, A. De Roeck, M.M. Defranchis, M. Deile, M. Dobson, M. Dünser, N. Dupont, F. Fallavollita[60], A. Florent, L. Forthomme, G. Franzoni, W. Funk, S. Ghosh[61], S. Giani, D. Gigi, K. Gill, F. Glege, L. Gouskos, E. Govorkova, M. Haranko, J. Hegeman, V. Innocente, T. James, P. Janot, J. Kaspar, J. Kieseler, N. Kratochwil, S. Laurila, P. Lecoq, E. Leutgeb, C. Lourenço, B. Maier, L. Malgeri, M. Mannelli, A.C. Marini, F. Meijers, S. Mersi, E. Meschi, F. Moortgat, M. Mulders, S. Orfanelli, L. Orsini, F. Pantaleo, E. Perez, M. Peruzzi, A. Petrilli, G. Petrucciani, A. Pfeiffer, M. Pierini, D. Piparo, M. Pitt, H. Qu, T. Quast, D. Rabady, A. Racz, G. Reales Gutiérrez, M. Rovere, H. Sakulin, J. Salfeld-Nebgen, S. Scarfi, M. Selvaggi, A. Sharma, P. Silva, P. Sphicas[62], A.G. Stahl Leiton, S. Summers, K. Tatar, D. Treille, P. Tropea, A. Tsirou, D. Walter, J. Wanczyk[63], K.A. Wozniak, W.D. Zeuner

Paul Scherrer Institut, Villigen, Switzerland

T. Bevilacqua[64], L. Caminada[64], A. Ebrahimi, W. Erdmann, R. Horisberger, Q. Ingram, H.C. Kaestli, D. Kotlinski, C. Lange, M. Missiroli[64], L. Noehte[64], T. Rohe

ETH Zurich — Institute for Particle Physics and Astrophysics (IPA), Zurich, Switzerland

T.K. Aarrestad, K. Androsov[63], M. Backhaus, A. Calandri, K. Datta, A. De Cosa, G. Dissertori, M. Dittmar, M. Donegà, F. Eble, M. Galli, K. Gedia, F. Glessgen, T.A. Gómez Espinosa, C. Grab, D. Hits, W. Lustermann, A.-M. Lyon, R.A. Manzoni, L. Marchese, C. Martin Perez, A. Mascellani[63], F. Nessi-Tedaldi, J. Niedziela, F. Pauss, V. Perovic, S. Pigazzini, M.G. Ratti, M. Reichmann, C. Reissel, T. Reitenspiess, B. Ristic, F. Riti, D. Ruini, D.A. Sanz Becerra, R. Seidita, J. Steggemann[63], D. Valsecchi, R. Wallny

Universität Zürich, Zurich, Switzerland

C. Amsler[65], P. Bärtschi, C. Botta, D. Brzhechko, M.F. Canelli, K. Cormier, A. De Wit, R. Del Burgo, J.K. Heikkilä, M. Huwiler, W. Jin, A. Jofrehei, B. Kilminster, S. Leontsinis, S.P. Liechti, A. Macchiolo, P. Meiring, V.M. Mikuni, U. Molinatti, I. Neutelings, A. Reimers, P. Robmann, S. Sanchez Cruz, K. Schweiger, M. Senger, Y. Takahashi

National Central University, Chung-Li, Taiwan

C. Adloff[66], C.M. Kuo, W. Lin, P.K. Rout, P.C. Tiwari[37], S.S. Yu

National Taiwan University (NTU), Taipei, Taiwan

L. Ceard, Y. Chao, K.F. Chen, P.s. Chen, H. Cheng, W.-S. Hou, R. Khurana, G. Kole, Y.y. Li, R.-S. Lu, E. Paganis, A. Psallidas, A. Steen, H.y. Wu, E. Yazgan

Chulalongkorn University, Faculty of Science, Department of Physics, Bangkok, Thailand

C. Asawatangtrakuldee, N. Srimanobhas, V. Wachirapusitanand

JHEP01(2024)128

Çukurova University, Physics Department, Science and Art Faculty, Adana, Turkey
D. Agyel, F. Boran, Z.S. Demiroglu, F. Dolek, I. Dumanoglu[67], E. Eskut, Y. Guler[68], E. Gurpinar Guler[68], C. Isik, O. Kara, A. Kayis Topaksu, U. Kiminsu, G. Onengut, K. Ozdemir[69], A. Polatoz, B. Tali[70], U.G. Tok, S. Turkcapar, E. Uslan, I.S. Zorbakir

Middle East Technical University, Physics Department, Ankara, Turkey
G. Karapinar[71], K. Ocalan[72], M. Yalvac[73]

Bogazici University, Istanbul, Turkey
B. Akgun, I.O. Atakisi, E. Gülmez, M. Kaya[74], O. Kaya[75], S. Tekten[76]

Istanbul Technical University, Istanbul, Turkey
A. Cakir, K. Cankocak[67], Y. Komurcu, S. Sen[77]

Istanbul University, Istanbul, Turkey
O. Aydilek, S. Cerci[70], V. Epshteyn, B. Hacisahinoglu, I. Hos[78], B. Isildak[79], B. Kaynak, S. Ozkorucuklu, C. Simsek, D. Sunar Cerci[70]

Institute for Scintillation Materials of National Academy of Science of Ukraine, Kharkiv, Ukraine
B. Grynyov

National Science Centre, Kharkiv Institute of Physics and Technology, Kharkiv, Ukraine
L. Levchuk

University of Bristol, Bristol, United Kingdom
D. Anthony, J.J. Brooke, A. Bundock, E. Clement, D. Cussans, H. Flacher, M. Glowacki, J. Goldstein, H.F. Heath, L. Kreczko, B. Krikler, S. Paramesvaran, S. Seif El Nasr-Storey, V.J. Smith, N. Stylianou[80], K. Walkingshaw Pass, R. White

Rutherford Appleton Laboratory, Didcot, United Kingdom
A.H. Ball, K.W. Bell, A. Belyaev[81], C. Brew, R.M. Brown, D.J.A. Cockerill, C. Cooke, K.V. Ellis, K. Harder, S. Harper, M.-L. Holmberg[82], Sh. Jain, J. Linacre, K. Manolopoulos, D.M. Newbold, E. Olaiya, D. Petyt, T. Reis, G. Salvi, T. Schuh, C.H. Shepherd-Themistocleous, I.R. Tomalin, T. Williams

Imperial College, London, United Kingdom
R. Bainbridge, P. Bloch, S. Bonomally, J. Borg, C.E. Brown, O. Buchmuller, V. Cacchio, C.A. Carrillo Montoya, V. Cepaitis, G.S. Chahal[83], D. Colling, J.S. Dancu, P. Dauncey, G. Davies, J. Davies, M. Della Negra, S. Fayer, G. Fedi, G. Hall, M.H. Hassanshahi, A. Howard, G. Iles, J. Langford, L. Lyons, A.-M. Magnan, S. Malik, A. Martelli, M. Mieskolainen, D.G. Monk, J. Nash[84], M. Pesaresi, B.C. Radburn-Smith, A. Richards, A. Rose, E. Scott, C. Seez, R. Shukla, A. Tapper, K. Uchida, G.P. Uttley, L.H. Vage, T. Virdee[26], M. Vojinovic, N. Wardle, S.N. Webb, D. Winterbottom

JHEP01(2024)128

Brunel University, Uxbridge, United Kingdom
K. Coldham, J.E. Cole, A. Khan, P. Kyberd, I.D. Reid

Baylor University, Waco, Texas, U.S.A.
S. Abdullin, A. Brinkerhoff, B. Caraway, J. Dittmann, K. Hatakeyama, J. Hiltbrand, A.R. Kanuganti, B. McMaster, M. Saunders, S. Sawant, C. Sutantawibul, M. Toms, J. Wilson

Catholic University of America, Washington, DC, U.S.A.
R. Bartek, A. Dominguez, C. Huerta Escamilla, A.E. Simsek, R. Uniyal, A.M. Vargas Hernandez

The University of Alabama, Tuscaloosa, Alabama, U.S.A.
R. Chudasama, S.I. Cooper, D. Di Croce, S.V. Gleyzer, C.U. Perez, P. Rumerio[85], E. Usai, C. West

Boston University, Boston, Massachusetts, U.S.A.
A. Akpinar, A. Albert, D. Arcaro, C. Cosby, Z. Demiragli, C. Erice, E. Fontanesi, D. Gastler, S. May, J. Rohlf, K. Salyer, D. Sperka, D. Spitzbart, I. Suarez, A. Tsatsos, S. Yuan

Brown University, Providence, Rhode Island, U.S.A.
G. Benelli, X. Coubez[21], D. Cutts, M. Hadley, U. Heintz, J.M. Hogan[86], T. Kwon, G. Landsberg, K.T. Lau, D. Li, J. Luo, M. Narain, N. Pervan, S. Sagir[87], F. Simpson, W.Y. Wong, X. Yan, D. Yu, W. Zhang

University of California, Davis, Davis, California, U.S.A.
S. Abbott, J. Bonilla, C. Brainerd, R. Breedon, M. Calderon De La Barca Sanchez, M. Chertok, J. Conway, P.T. Cox, R. Erbacher, G. Haza, F. Jensen, O. Kukral, G. Mocellin, M. Mulhearn, D. Pellett, B. Regnery, W. Wei, Y. Yao, F. Zhang

University of California, Los Angeles, California, U.S.A.
M. Bachtis, R. Cousins, A. Datta, J. Hauser, M. Ignatenko, M.A. Iqbal, T. Lam, E. Manca, W.A. Nash, D. Saltzberg, B. Stone, V. Valuev

University of California, Riverside, Riverside, California, U.S.A.
R. Clare, J.W. Gary, M. Gordon, G. Hanson, O.R. Long, N. Manganelli, W. Si, S. Wimpenny

University of California, San Diego, La Jolla, California, U.S.A.
J.G. Branson, S. Cittolin, S. Cooperstein, D. Diaz, J. Duarte, R. Gerosa, L. Giannini, J. Guiang, R. Kansal, V. Krutelyov, R. Lee, J. Letts, M. Masciovecchio, F. Mokhtar, M. Pieri, M. Quinnan, B.V. Sathia Narayanan, V. Sharma, M. Tadel, E. Vourliotis, F. Würthwein, Y. Xiang, A. Yagil

JHEP01(2024)128

University of California, Santa Barbara — Department of Physics, Santa Barbara, California, U.S.A.

L. Brennan, C. Campagnari, M. Citron, G. Collura, A. Dorsett, J. Incandela, M. Kilpatrick, J. Kim, A.J. Li, P. Masterson, H. Mei, M. Oshiro, J. Richman, U. Sarica, R. Schmitz, F. Setti, J. Sheplock, P. Siddireddy, D. Stuart, S. Wang

California Institute of Technology, Pasadena, California, U.S.A.

A. Bornheim, O. Cerri, A. Latorre, J.M. Lawhorn, J. Mao, H.B. Newman, T. Q. Nguyen, M. Spiropulu, J.R. Vlimant, C. Wang, S. Xie, R.Y. Zhu

Carnegie Mellon University, Pittsburgh, Pennsylvania, U.S.A.

J. Alison, S. An, M.B. Andrews, P. Bryant, V. Dutta, T. Ferguson, A. Harilal, C. Liu, T. Mudholkar, S. Murthy, M. Paulini, A. Roberts, A. Sanchez, W. Terrill

University of Colorado Boulder, Boulder, Colorado, U.S.A.

J.P. Cumalat, W.T. Ford, A. Hassani, G. Karathanasis, E. MacDonald, F. Marini, A. Perloff, C. Savard, N. Schonbeck, K. Stenson, K.A. Ulmer, S.R. Wagner, N. Zipper

Cornell University, Ithaca, New York, U.S.A.

J. Alexander, S. Bright-Thonney, X. Chen, D.J. Cranshaw, J. Fan, X. Fan, D. Gadkari, S. Hogan, J. Monroy, J.R. Patterson, J. Reichert, M. Reid, A. Ryd, J. Thom, P. Wittich, R. Zou

Fermi National Accelerator Laboratory, Batavia, Illinois, U.S.A.

M. Albrow, M. Alyari, O. Amram, G. Apollinari, A. Apresyan, L.A.T. Bauerdick, D. Berry, J. Berryhill, P.C. Bhat, K. Burkett, J.N. Butler, A. Canepa, G.B. Cerati, H.W.K. Cheung, F. Chlebana, K.F. Di Petrillo, J. Dickinson, I. Dutta, V.D. Elvira, Y. Feng, J. Freeman, A. Gandrakota, Z. Gecse, L. Gray, D. Green, S. Grünendahl, D. Guerrero, O. Gutsche, R.M. Harris, R. Heller, T.C. Herwig, J. Hirschauer, L. Horyn, B. Jayatilaka, S. Jindariani, M. Johnson, U. Joshi, T. Klijnsma, B. Klima, K.H.M. Kwok, S. Lammel, D. Lincoln, R. Lipton, T. Liu, C. Madrid, K. Maeshima, C. Mantilla, D. Mason, P. McBride, P. Merkel, S. Mrenna, S. Nahn, J. Ngadiuba, D. Noonan, S. Norberg, V. Papadimitriou, N. Pastika, K. Pedro, C. Pena[88], F. Ravera, A. Reinsvold Hall[89], L. Ristori, E. Sexton-Kennedy, N. Smith, A. Soha, L. Spiegel, J. Strait, L. Taylor, S. Tkaczyk, N.V. Tran, L. Uplegger, E.W. Vaandering, I. Zoi

University of Florida, Gainesville, Florida, U.S.A.

P. Avery, D. Bourilkov, L. Cadamuro, P. Chang, V. Cherepanov, R.D. Field, E. Koenig, M. Kolosova, J. Konigsberg, A. Korytov, E. Kuznetsova[90], K.H. Lo, K. Matchev, N. Menendez, G. Mitselmakher, A. Muthirakalayil Madhu, N. Rawal, D. Rosenzweig, S. Rosenzweig, K. Shi, J. Wang, Z. Wu

Florida State University, Tallahassee, Florida, U.S.A.

T. Adams, A. Askew, N. Bower, R. Habibullah, V. Hagopian, T. Kolberg, G. Martinez, H. Prosper, O. Viazlo, M. Wulansatiti, R. Yohay, J. Zhang

JHEP01(2024)128

Florida Institute of Technology, Melbourne, Florida, U.S.A.
M.M. Baarmand, S. Butalla, T. Elkafrawy[52], M. Hohlmann, R. Kumar Verma, M. Rahmani, F. Yumiceva

University of Illinois at Chicago (UIC), Chicago, Illinois, U.S.A.
M.R. Adams, R. Cavanaugh, S. Dittmer, O. Evdokimov, C.E. Gerber, D.J. Hofman, D. S. Lemos, A.H. Merrit, C. Mills, G. Oh, T. Roy, S. Rudrabhatla, M.B. Tonjes, N. Varelas, X. Wang, Z. Ye, J. Yoo

The University of Iowa, Iowa City, Iowa, U.S.A.
M. Alhusseini, K. Dilsiz[91], L. Emediato, G. Karaman, O.K. Köseyan, J.-P. Merlo, A. Mestvirishvili[92], J. Nachtman, O. Neogi, H. Ogul[93], Y. Onel, A. Penzo, C. Snyder, E. Tiras[94]

Johns Hopkins University, Baltimore, Maryland, U.S.A.
B. Blumenfeld, L. Corcodilos, J. Davis, A.V. Gritsan, S. Kyriacou, P. Maksimovic, J. Roskes, S. Sekhar, M. Swartz, T.Á. Vámi

The University of Kansas, Lawrence, Kansas, U.S.A.
A. Abreu, L.F. Alcerro Alcerro, J. Anguiano, P. Baringer, A. Bean, Z. Flowers, J. King, G. Krintiras, M. Lazarovits, C. Le Mahieu, C. Lindsey, J. Marquez, N. Minafra, M. Murray, M. Nickel, C. Rogan, C. Royon, R. Salvatico, S. Sanders, C. Smith, Q. Wang, G. Wilson

Kansas State University, Manhattan, Kansas, U.S.A.
B. Allmond, S. Duric, A. Ivanov, K. Kaadze, A. Kalogeropoulos, D. Kim, Y. Maravin, T. Mitchell, A. Modak, K. Nam, D. Roy

Lawrence Livermore National Laboratory, Livermore, California, U.S.A.
F. Rebassoo, D. Wright

University of Maryland, College Park, Maryland, U.S.A.
E. Adams, A. Baden, O. Baron, A. Belloni, A. Bethani, Y.m. Chen, S.C. Eno, N.J. Hadley, S. Jabeen, R.G. Kellogg, T. Koeth, Y. Lai, S. Lascio, A.C. Mignerey, S. Nabili, C. Palmer, C. Papageorgakis, L. Wang, K. Wong

Massachusetts Institute of Technology, Cambridge, Massachusetts, U.S.A.
J. Bendavid, W. Busza, I.A. Cali, Y. Chen, M. D'Alfonso, J. Eysermans, C. Freer, G. Gomez-Ceballos, M. Goncharov, P. Harris, D. Kovalskyi, J. Krupa, Y.-J. Lee, K. Long, C. Mironov, C. Paus, D. Rankin, C. Roland, G. Roland, Z. Shi, G.S.F. Stephans, J. Wang, Z. Wang, B. Wyslouch, T. J. Yang

University of Minnesota, Minneapolis, Minnesota, U.S.A.
R.M. Chatterjee, B. Crossman, B.M. Joshi, C. Kapsiak, M. Krohn, Y. Kubota, D. Mahon, J. Mans, M. Revering, R. Rusack, R. Saradhy, N. Schroeder, N. Strobbe, M.A. Wadud

JHEP01(2024)128

University of Mississippi, Oxford, Mississippi, U.S.A.
L.M. Cremaldi

University of Nebraska-Lincoln, Lincoln, Nebraska, U.S.A.
K. Bloom, M. Bryson, D.R. Claes, C. Fangmeier, F. Golf, C. Joo, I. Kravchenko, I. Reed, J.E. Siado, G.R. Snow†, W. Tabb, A. Wightman, F. Yan, A.G. Zecchinelli

State University of New York at Buffalo, Buffalo, New York, U.S.A.
G. Agarwal, H. Bandyopadhyay, L. Hay, I. Iashvili, A. Kharchilava, C. McLean, M. Morris, D. Nguyen, J. Pekkanen, S. Rappoccio, H. Rejeb Sfar, A. Williams

Northeastern University, Boston, Massachusetts, U.S.A.
G. Alverson, E. Barberis, Y. Haddad, Y. Han, A. Krishna, J. Li, J. Lidrych, G. Madigan, B. Marzocchi, D.M. Morse, V. Nguyen, T. Orimoto, A. Parker, L. Skinnari, A. Tishelman-Charny, T. Wamorkar, B. Wang, A. Wisecarver, D. Wood

Northwestern University, Evanston, Illinois, U.S.A.
S. Bhattacharya, J. Bueghly, Z. Chen, A. Gilbert, K.A. Hahn, Y. Liu, N. Odell, M.H. Schmitt, M. Velasco

University of Notre Dame, Notre Dame, Indiana, U.S.A.
R. Band, R. Bucci, M. Cremonesi, A. Das, R. Goldouzian, M. Hildreth, K. Hurtado Anampa, C. Jessop, K. Lannon, J. Lawrence, N. Loukas, L. Lutton, J. Mariano, N. Marinelli, I. Mcalister, T. McCauley, C. Mcgrady, K. Mohrman, C. Moore, Y. Musienko[12], R. Ruchti, A. Townsend, M. Wayne, H. Yockey, M. Zarucki, L. Zygala

The Ohio State University, Columbus, Ohio, U.S.A.
B. Bylsma, M. Carrigan, L.S. Durkin, C. Hill, M. Joyce, A. Lesauvage, M. Nunez Ornelas, K. Wei, B.L. Winer, B. R. Yates

Princeton University, Princeton, New Jersey, U.S.A.
F.M. Addesa, H. Bouchamaoui, P. Das, G. Dezoort, P. Elmer, A. Frankenthal, B. Greenberg, N. Haubrich, S. Higginbotham, G. Kopp, S. Kwan, D. Lange, A. Loeliger, D. Marlow, I. Ojalvo, J. Olsen, D. Stickland, C. Tully

University of Puerto Rico, Mayaguez, Puerto Rico, U.S.A.
S. Malik

Purdue University, West Lafayette, Indiana, U.S.A.
A.S. Bakshi, V.E. Barnes, J. Bertaux, S. Chandra, R. Chawla, S. Das, L. Gutay, M. Jones, A.W. Jung, D. Kondratyev, A.M. Koshy, M. Liu, G. Negro, N. Neumeister, G. Paspalaki, S. Piperov, A. Purohit, J.F. Schulte, M. Stojanovic[15], J. Thieman, A. K. Virdi, F. Wang, R. Xiao, W. Xie

Purdue University Northwest, Hammond, Indiana, U.S.A.
J. Dolen, N. Parashar

Rice University, Houston, Texas, U.S.A.
D. Acosta, A. Baty, T. Carnahan, S. Dildick, K.M. Ecklund, P.J. Fernández Manteca, S. Freed, P. Gardner, F.J.M. Geurts, A. Kumar, W. Li, O. Miguel Colin, B.P. Padley, R. Redjimi, J. Rotter, S. Yang, E. Yigitbasi, Y. Zhang

University of Rochester, Rochester, New York, U.S.A.
A. Bodek, P. de Barbaro, R. Demina, J.L. Dulemba, C. Fallon, A. Garcia-Bellido, O. Hindrichs, A. Khukhunaishvili, P. Parygin, E. Popova, R. Taus, G.P. Van Onsem

The Rockefeller University, New York, New York, U.S.A.
K. Goulianos

Rutgers, The State University of New Jersey, Piscataway, New Jersey, U.S.A.
B. Chiarito, J.P. Chou, Y. Gershtein, E. Halkiadakis, A. Hart, M. Heindl, D. Jaroslawski, O. Karacheban[24], I. Laflotte, A. Lath, R. Montalvo, K. Nash, M. Osherson, H. Routray, S. Salur, S. Schnetzer, S. Somalwar, R. Stone, S.A. Thayil, S. Thomas, J. Vora, H. Wang

University of Tennessee, Knoxville, Tennessee, U.S.A.
H. Acharya, A.G. Delannoy, S. Fiorendi, T. Holmes, E. Nibigira, S. Spanier

Texas A&M University, College Station, Texas, U.S.A.
M. Ahmad, O. Bouhali[95], M. Dalchenko, A. Delgado, R. Eusebi, J. Gilmore, T. Huang, T. Kamon[96], H. Kim, S. Luo, S. Malhotra, R. Mueller, D. Overton, D. Rathjens, A. Safonov

Texas Tech University, Lubbock, Texas, U.S.A.
N. Akchurin, J. Damgov, V. Hegde, K. Lamichhane, S.W. Lee, T. Mengke, S. Muthumuni, T. Peltola, I. Volobouev, A. Whitbeck

Vanderbilt University, Nashville, Tennessee, U.S.A.
E. Appelt, S. Greene, A. Gurrola, W. Johns, R. Kunnawalkam Elayavalli, A. Melo, F. Romeo, P. Sheldon, S. Tuo, J. Velkovska, J. Viinikainen

University of Virginia, Charlottesville, Virginia, U.S.A.
B. Cardwell, B. Cox, G. Cummings, J. Hakala, R. Hirosky, A. Ledovskoy, A. Li, C. Neu, C.E. Perez Lara

Wayne State University, Detroit, Michigan, U.S.A.
P.E. Karchin

University of Wisconsin — Madison, Madison, Wisconsin, U.S.A.
A. Aravind, S. Banerjee, K. Black, T. Bose, S. Dasu, I. De Bruyn, P. Everaerts, C. Galloni, H. He, M. Herndon, A. Herve, C.K. Koraka, A. Lanaro, R. Loveless, J. Madhusudanan Sreekala, A. Mallampalli, A. Mohammadi, S. Mondal, G. Parida,

JHEP01(2024)128

D. Pinna, A. Savin, V. Shang, V. Sharma, W.H. Smith, D. Teague, H.F. Tsoi, W. Vetens, A. Warden

Authors affiliated with an institute or an international laboratory covered by a cooperation agreement with CERN

S. Afanasiev, V. Andreev, Yu. Andreev, T. Aushev, M. Azarkin, A. Babaev, A. Belyaev, V. Blinov[97], E. Boos, V. Borshch, D. Budkouski, V. Chekhovsky, R. Chistov[97], M. Danilov[97], A. Dermenev, T. Dimova[97], I. Dremin, A. Ershov, G. Gavrilov, V. Gavrilov, S. Gninenko, V. Golovtcov, N. Golubev, I. Golutvin, I. Gorbunov, A. Gribushin, Y. Ivanov, V. Kachanov, A. Kaminskiy, L. Kardapoltsev[97], V. Karjavine, A. Karneyeu, L. Khein, V. Kim[97], M. Kirakosyan, D. Kirpichnikov, M. Kirsanov, O. Kodolova[98], D. Konstantinov, V. Korenkov, V. Korotkikh, A. Kozyrev[97], N. Krasnikov, A. Lanev, P. Levchenko[99], A. Litomin, N. Lychkovskaya, V. Makarenko, A. Malakhov, V. Matveev[97], V. Murzin, A. Nikitenko[100,98], S. Obraztsov, I. Ovtin[97], V. Palichik, V. Perelygin, S. Petrushanko, S. Polikarpov[97], V. Popov, O. Radchenko[97], M. Savina, V. Savrin, D. Selivanova, V. Shalaev, S. Shmatov, S. Shulha, Y. Skovpen[97], S. Slabospitskii, V. Smirnov, A. Snigirev, D. Sosnov, V. Sulimov, E. Tcherniaev, A. Terkulov, O. Teryaev, I. Tlisova, A. Toropin, L. Uvarov, A. Uzunian, I. Vardanyan, A. Vorobyev[†], N. Voytishin, B.S. Yuldashev[101], A. Zarubin, I. Zhizhin, A. Zhokin

[†] *Deceased*
[1] *Also at Yerevan State University, Yerevan, Armenia*
[2] *Also at TU Wien, Vienna, Austria*
[3] *Also at Institute of Basic and Applied Sciences, Faculty of Engineering, Arab Academy for Science, Technology and Maritime Transport, Alexandria, Egypt*
[4] *Also at Université Libre de Bruxelles, Bruxelles, Belgium*
[5] *Also at Universidade Estadual de Campinas, Campinas, Brazil*
[6] *Also at Federal University of Rio Grande do Sul, Porto Alegre, Brazil*
[7] *Also at UFMS, Nova Andradina, Brazil*
[8] *Also at University of Chinese Academy of Sciences, Beijing, China*
[9] *Also at Nanjing Normal University, Nanjing, China*
[10] *Now at The University of Iowa, Iowa City, Iowa, U.S.A.*
[11] *Also at University of Chinese Academy of Sciences, Beijing, China*
[12] *Also at an institute or an international laboratory covered by a cooperation agreement with CERN*
[13] *Also at Suez University, Suez, Egypt*
[14] *Now at British University in Egypt, Cairo, Egypt*
[15] *Also at Purdue University, West Lafayette, Indiana, U.S.A.*
[16] *Also at Université de Haute Alsace, Mulhouse, France*
[17] *Also at Department of Physics, Tsinghua University, Beijing, China*
[18] *Also at The University of the State of Amazonas, Manaus, Brazil*
[19] *Also at Erzincan Binali Yildirim University, Erzincan, Turkey*
[20] *Also at University of Hamburg, Hamburg, Germany*
[21] *Also at RWTH Aachen University, III. Physikalisches Institut A, Aachen, Germany*
[22] *Also at Isfahan University of Technology, Isfahan, Iran*
[23] *Also at Bergische University Wuppertal (BUW), Wuppertal, Germany*
[24] *Also at Brandenburg University of Technology, Cottbus, Germany*
[25] *Also at Forschungszentrum Jülich, Juelich, Germany*
[26] *Also at CERN, European Organization for Nuclear Research, Geneva, Switzerland*
[27] *Also at Physics Department, Faculty of Science, Assiut University, Assiut, Egypt*
[28] *Also at Wigner Research Centre for Physics, Budapest, Hungary*

JHEP01(2024)128

[29] Also at Institute of Physics, University of Debrecen, Debrecen, Hungary
[30] Also at Institute of Nuclear Research ATOMKI, Debrecen, Hungary
[31] Now at Universitatea Babes-Bolyai — Facultatea de Fizica, Cluj-Napoca, Romania
[32] Also at Faculty of Informatics, University of Debrecen, Debrecen, Hungary
[33] Also at Punjab Agricultural University, Ludhiana, India
[34] Also at UPES — University of Petroleum and Energy Studies, Dehradun, India
[35] Also at University of Visva-Bharati, Santiniketan, India
[36] Also at University of Hyderabad, Hyderabad, India
[37] Also at Indian Institute of Science (IISc), Bangalore, India
[38] Also at Indian Institute of Technology (IIT), Mumbai, India
[39] Also at IIT Bhubaneswar, Bhubaneswar, India
[40] Also at Institute of Physics, Bhubaneswar, India
[41] Also at Deutsches Elektronen-Synchrotron, Hamburg, Germany
[42] Now at Department of Physics, Isfahan University of Technology, Isfahan, Iran
[43] Also at Sharif University of Technology, Tehran, Iran
[44] Also at Department of Physics, University of Science and Technology of Mazandaran, Behshahr, Iran
[45] Also at Helwan University, Cairo, Egypt
[46] Also at Italian National Agency for New Technologies, Energy and Sustainable Economic Development, Bologna, Italy
[47] Also at Centro Siciliano di Fisica Nucleare e di Struttura Della Materia, Catania, Italy
[48] Also at Università degli Studi Guglielmo Marconi, Roma, Italy
[49] Also at Scuola Superiore Meridionale, Università di Napoli 'Federico II', Napoli, Italy
[50] Also at Fermi National Accelerator Laboratory, Batavia, Illinois, U.S.A.
[51] Also at Università di Napoli 'Federico II', Napoli, Italy
[52] Also at Ain Shams University, Cairo, Egypt
[53] Also at Consiglio Nazionale delle Ricerche — Istituto Officina dei Materiali, Perugia, Italy
[54] Also at Riga Technical University, Riga, Latvia
[55] Also at Department of Applied Physics, Faculty of Science and Technology, Universiti Kebangsaan Malaysia, Bangi, Malaysia
[56] Also at Consejo Nacional de Ciencia y Tecnología, Mexico City, Mexico
[57] Also at IRFU, CEA, Université Paris-Saclay, Gif-sur-Yvette, France
[58] Also at Faculty of Physics, University of Belgrade, Belgrade, Serbia
[59] Also at Trincomalee Campus, Eastern University, Sri Lanka, Nilaveli, Sri Lanka
[60] Also at INFN Sezione di Pavia, Università di Pavia, Pavia, Italy
[61] Also at Indian Institute of Technology Hyderabad, Hyderabad, India
[62] Also at National and Kapodistrian University of Athens, Athens, Greece
[63] Also at Ecole Polytechnique Fédérale Lausanne, Lausanne, Switzerland
[64] Also at Universität Zürich, Zurich, Switzerland
[65] Also at Stefan Meyer Institute for Subatomic Physics, Vienna, Austria
[66] Also at Laboratoire d'Annecy-le-Vieux de Physique des Particules, IN2P3-CNRS, Annecy-le-Vieux, France
[67] Also at Near East University, Research Center of Experimental Health Science, Mersin, Turkey
[68] Also at Konya Technical University, Konya, Turkey
[69] Also at Izmir Bakircay University, Izmir, Turkey
[70] Also at Adiyaman University, Adiyaman, Turkey
[71] Also at Istanbul Gedik University, Istanbul, Turkey
[72] Also at Necmettin Erbakan University, Konya, Turkey
[73] Also at Bozok Universitetesi Rektörlügü, Yozgat, Turkey
[74] Also at Marmara University, Istanbul, Turkey
[75] Also at Milli Savunma University, Istanbul, Turkey
[76] Also at Kafkas University, Kars, Turkey
[77] Also at Hacettepe University, Ankara, Turkey
[78] Also at Istanbul University — Cerrahpasa, Faculty of Engineering, Istanbul, Turkey
[79] Also at Yildiz Technical University, Istanbul, Turkey

JHEP01(2024)128

[80] *Also at Vrije Universiteit Brussel, Brussel, Belgium*
[81] *Also at School of Physics and Astronomy, University of Southampton, Southampton, United Kingdom*
[82] *Also at University of Bristol, Bristol, United Kingdom*
[83] *Also at IPPP Durham University, Durham, United Kingdom*
[84] *Also at Monash University, Faculty of Science, Clayton, Australia*
[85] *Also at Università di Torino, Torino, Italy*
[86] *Also at Bethel University, St. Paul, Minnesota, U.S.A.*
[87] *Also at Karamanoğlu Mehmetbey University, Karaman, Turkey*
[88] *Also at California Institute of Technology, Pasadena, California, U.S.A.*
[89] *Also at United States Naval Academy, Annapolis, Maryland, U.S.A.*
[90] *Also at University of Florida, Gainesville, Florida, U.S.A.*
[91] *Also at Bingol University, Bingol, Turkey*
[92] *Also at Georgian Technical University, Tbilisi, Georgia*
[93] *Also at Sinop University, Sinop, Turkey*
[94] *Also at Erciyes University, Kayseri, Turkey*
[95] *Also at Texas A&M University at Qatar, Doha, Qatar*
[96] *Also at Kyungpook National University, Daegu, Korea*
[97] *Also at another institute or international laboratory covered by a cooperation agreement with CERN*
[98] *Also at Yerevan Physics Institute, Yerevan, Armenia*
[99] *Also at Northeastern University, Boston, Massachusetts, U.S.A.*
[100] *Also at Imperial College, London, United Kingdom*
[101] *Also at Institute of Nuclear Physics of the Uzbekistan Academy of Sciences, Tashkent, Uzbekistan*

JHEP01(2024)128